Survivin-Induced Abnormal Ploidy Contributes to Cystic Kidney and Aneurysm Formation

Wissam A. AbouAlaiwi, PhD*; Brian S. Muntean, BSc*; Shobha Ratnam, MD, PhD; Bina Joe, PhD; Lijun Liu, MD; Robert L. Booth, MD; Ingrid Rodriguez, DO; Britney S. Herbert, PhD; Robert L. Bacallao, MD; Marcus Fruttiger, PhD; Tak W. Mak, PhD; Jing Zhou, MD, PhD; Surya M. Nauli, PhD

Background—Cystic kidneys and vascular aneurysms are clinical manifestations seen in patients with polycystic kidney disease, a cilia-associated pathology (ciliopathy). Survivin overexpression is associated with cancer, but the clinical pathology associated with survivin downregulation or knockout has never been studied before. The present studies aim to examine whether and how cilia function (*Pkd1* or *Pkd2*) and structure (*Tg737*) play a role in cystic kidney and aneurysm through survivin downregulation.

Methods and Results—Cysts and aneurysms from polycystic kidney disease patients, *Pkd* mouse, and zebrafish models are characterized by chromosome instability and low survivin expression. This triggers cytokinesis defects and formation of nuclear polyploidy or aneuploidy. In vivo conditional mouse and zebrafish models confirm that *survivin* gene deletion in the kidneys results in a cystic phenotype. As in hypertensive *Pkd1*, *Pkd2*, and *Tg737* models, aneurysm formation can also be induced in vascular-specific normotensive *survivin* mice. *Survivin* knockout also contributes to abnormal oriented cell division in both kidney and vasculature. Furthermore, survivin expression and ciliary localization are regulated by flow-induced cilia activation through protein kinase C, Akt and nuclear factor-κB. Circumventing ciliary function by re-expressing survivin can rescue polycystic kidney disease phenotypes.

Conclusions—For the first time, our studies offer a unifying mechanism that explains both renal and vascular phenotypes in polycystic kidney disease. Although primary cilia dysfunction accounts for aneurysm formation and hypertension, hypertension itself does not cause aneurysm. Furthermore, aneurysm formation and cyst formation share a common cellular and molecular pathway involving cilia function or structure, survivin expression, cytokinesis, cell ploidy, symmetrical cell division, and tissue architecture orientation. **(*Circulation*. 2014;129:660-672.)**

Key Words: aurora kinase ■ blood flow ■ blood pressure ■ cardiovascular system ■ epithelium ■ endothelium, vascular

Polycystic kidney disease (PKD) is the most common hereditary kidney disorder, and formation of bilateral cystic kidneys is the hallmark of the disease. Among other extrarenal phenotypes, aneurysm formation is one of the deadliest vascular abnormalities observed in PKD patients. Unfortunately, there is no study that explains the formation of these "bulb-like structures" in both vasculatures and renal tubules. Abnormalities in primary cilia,[1–4] polyploidy,[5,6] and centrosomal number[5,7] have been independently studied in the vascular or renal systems. However, there is currently no unifying mechanism that explains these cellular phenotypes.

Clinical Perspective on p 672

Survivin is a chromosomal passenger involved in coordinating proper chromosomal events during mitosis.[8] Because of its clinical manifestation in cancer, overexpression of survivin has always been the main focus of medical research. Whereas overexpression of survivin is associated with cancer formation and progression, the *Survivin* knockout mouse model is not viable beyond 4.5 days post coitum.[9] Interestingly, *survivin* homozygote cells isolated at 4.5 days post coitum show a cellular polyploidy phenotype similar to that of *Pkd* cells.

Received June 17, 2013; accepted October 28, 2013.

From the Department of Pharmacology (W.A.A., S.M.N.), Department of Medicinal and Biological Chemistry (B.S.M., S.M.N.), Department of Medicine (S.R., S.M.N.), Center for Hypertension and Personalized Medicine (B.J., S.M.N.), Department of Biochemistry and Cancer Biology (L.L.), and Department of Pathology (R.L.B.), University of Toledo, Toledo, OH; Department of Emergency and Intensive Care, ProMedica Sponsored Research, Toledo, OH (I.R.); Departments of Medicine (B.S.H.) and Medical and Molecular Genetics (R.L.B.), Indiana University School of Medicine, Indianapolis; UCL Institute of Ophthalmology, University College London, London, UK (M.F.); Ontario Cancer Institute, University Health Network, Toronto, ON, Canada (T.W.M.); and Department of Medicine, Brigham and Women's Hospital, Boston, MA (J.Z.).

Guest Editor for this article was Donald D. Heistad, MD.

*Dr AbouAlaiwi and B.S. Muntean contributed equally.

The online-only Data Supplement is available with this article at http://circ.ahajournals.org/lookup/suppl/doi:10.1161/CIRCULATIONAHA.113.005746/-/DC1.

Correspondence to Surya M. Nauli, PhD, University of Toledo, Department of Pharmacology, MS No. 1015, Health Education Bldg, Room 274, 3000 Arlington Ave, Toledo, OH 43614. E-mail Surya.Nauli@UToledo.Edu

Our previous in vitro studies showed that vascular endothelial *Pkd* cell lines are characterized by survivin downregulation, resulting in abnormal spindle assembly checkpoint and polyploidy.[5] Here, we expanded our study through the use of in vivo mouse and zebrafish models to demonstrate that survivin knockout or knockdown is sufficient to induce the formation of bulb-like structures in the kidney tubule (cysts) and artery (aneurysms). Our studies further suggest that mechanosensory cilia regulate survivin expression and dictate the formation of cell ploidy. The asymmetrical cell division resulting from abnormal ploidy further undermines the establishment of tissue polarity or planar cell polarity, which is believed to be the underlying mechanism for tubule or artery dilatation. We thus propose a common cellular mechanism through survivin to explain both vascular and renal phenotypes in PKD.

Methods

Signed and informed consent to collect disposed human kidneys with PKD was obtained from the patients, and kidney collection protocols were approved by the Department for Human Research Protections of the Biomedical Institutional Review Board of the University of Toledo. The use of animal tissues was approved by the University of Toledo animal care and use committee.

Mouse Models

The following mouse models were used in our studies; *Mx1Cre, PdgfβCre, Tie2Cre, Pkd1^{flox}*, *Pkd2^{-}*, *Tg737^{Orpk}*, and *survivin^{flox}*. To accelerate the experimental cystic model, unilateral ureteral obstruction (UUO) was generated by tying a 6-0 silk suture against a 28G-gauge needle in the mice. Standard histology analyses were used to examine the kidneys. To accelerate experimental aneurysm formation, 0.25 mol/L calcium chloride was placed directly on the abdominal aorta of the mice for 10 minutes.

Cell Culture

Human and mouse primary tubular cells from distal collecting tubules were used in the present studies. For cell lines, we used previously generated mouse endothelial cells[3] and human renal epithelial cells.[4] In some experiments, human full-length survivin–green fluorescent protein was used, in addition to siRNA knockdown on protein kinase C (PKC), Akt, aurora-A, and survivin. These cells were then subjected to cell cycle, live imaging, karyotyping, immunostaining, or Western analysis.

Chromosomal Analysis

Chromosomes from a single cell were spread and hybridized with a cocktail of mouse or human fluorescence-labeled probes specific for individual chromosomes.[10] Data were analyzed with automated SKY View software (version 1.62). Because zebrafish chromosome-specific probes were not available, individual chromosomes were analyzed on the basis of the ideogram derived from the replication banding of *Danio rerio*.

Live Imaging study

Primary renal epithelial cells or vascular endothelial cells were transfected with or without *Survivin* siRNA. Hoechst dye was use to indicate the nucleus.

Zebrafish Study

Wild-type zebrafish AB strains were used for knockdown experiments with either control morpholino (*controlMO*: 5′-CCT CTT ACC TCA GTT ACA ATT TAT A-3′) or *Pkd2* morpholino (*pkd2MO:* 5′-AGG ACG AAC GCG ACT GGG CTC ATC-3′). For rescue experiments, 100 pg purified full-length human *survivin* mRNA was either coinjected with *pkd2* morpholinos or injected alone into the 1- to 2-cell-stage embryos. In another case, 2.5 ng vascular endothelial growth factor (VEGF) was coinjected with *pkd2* morpholinos.

RNA Isolation and Reverse Transcription–Polymerase Chain Reaction

Effectiveness of the knockdown or overexpression in zebrafish was verified by reverse transcription–polymerase chain reaction. Total RNA was isolated from zebrafish embryos with TRIzol (Invitrogen, Inc) followed by DNase treatment (Roche, Inc). Superscript-II (Invitrogen, Inc) was used for cDNA synthesis. Reverse transcription–polymerase chain reaction is performed under the following cycling conditions: 95°C for 15 minutes and then 40 cycles of 95°C for 30 seconds, 60°C for 1 minute, and 72°C for 1 minute. The cDNAs were amplified using specific primers indicated in the Table.[11–14]

Pharmacological Agents

The pharmacological agents used in our studies include PKC inhibitor (5 µmol/L Bisindolylmaleimide XI hydrochloride, Sigma Inc), PKC activator (10 µmol/L forskolin, Sigma Inc), taxol (33.3 nmol/L, Sigma, Inc), nocodazole (0.1 µg/mL, Sigma, Inc), VEGF (2.5 ng, Prospec, Inc), and colcemid (50 µg/mL, Invitrogen Inc).

Data Analysis

Both surgical and nonsurgical kidneys were studied and compared among the mouse groups. All quantifiable data were reported as mean±SEM. Distribution analyses were performed on all data sets before any statistical comparisons to confirm normal data distribution (a bell-shaped curve distribution). Homogeneity of variance (homoscedasticity) was also verified within each data set. When the data set was not normally distributed or heterogeneous variance was detected, the distributions were normalized by log transformation. This approach produced normally distributed data sets. After distribution and variance analyses, data comparisons for >2 groups were performed with ANOVA followed by the Dunn multiple-comparison posttest analysis. Comparison between 2 groups was carried out with the Student *t* test. Whenever possible, paired experimental design was used in our studies to allow more powerful statistical analysis and the use of fewer mice in each study group. For all comparisons, power analyses were performed routinely to enable reliable conclusions, and comparisons with negative results had statistical powers of ≥0.8. Unless otherwise indicated, the difference between groups was statistically significant at $P<0.05$, and

Table. Primer Sequences

Description	Primer Sequence	Reference
Zebrafish *pkd2*	Forward: 5′-GGG ATA CGT GCT GTG GTT CTC-3′ Reverse: 5′-CAC GAT GAG CTC CAG TCG CGT-3′	11
Human *survivin*	Forward: 5′-AAG AAC TGG CCC TTC TTG GA-3′ Reverse: 5′-CAA CCG GAC GAA TGC TTT TT-3′	12
Zebrafish *survivin*	Forward: 5′-GGA GCG ACT TCG CAT CTA CAT-3′ Reverse: 5′-ACC TCA TCA CGA AAG TAG GCA ATC-3′	13
Zebrafish α-*tubulin*	Forward: 5′-GGA GCT CAT TGA CCT TGT TTT AGA TA-3′ Reverse: 5′-GCT GTG GAA GAC CAG GAA ACC-3′	14

significance is indicated in the graphs by asterisks to denote comparison with the wild-type control, nontreated, noninduced, or static group. The number of experimental replicates is indicated in the figures or figure legends. All statistical analyses were done with GraphPad Prism, version 5.0.

Results

Human and Mouse Polycystic Kidneys Are Characterized by Abnormal Ploidy and Survivin Downregulation

Compared with noncystic tissue (Figure 1A), karyotyping data of a single renal epithelium from PKD patients showed an abnormal ploidy (Figure 1B). We consistently observed an astonishingly high abnormality in the genetic composition in the samples acquired from PKD patients (Figure 1C). We recently showed that survivin is downregulated in *Pkd*-derived mouse vascular endothelia.[5] We therefore examined survivin expression levels in our patients' samples. All freshly isolated kidney samples from PKD patients consistently show a downregulation in survivin expression (Figure 1D).

Survivin Downregulation Is Sufficient to Promote Cystic Kidney Ex Vivo and In Vivo

Because *Survivin* knockout mouse dies at 4.5 days post coitum,[9] we crossed *survivin-flox* mice with kidney-specific *Cre* mice (*Mx1Cre*). We also performed UUO surgery as a renal injury model to examine the relationship between renal injury and cyst formation. We inactivated survivin (*Mx1Cre:Survivin*$^{flox/flox}$) in 1-week-old mice and analyzed the cystic kidney phenotypes in 4-week-old (Figure 2A-i) and 3-month-old (Figure 2A-ii) mice. At 5-week-old mice, the effects of *Survivin* knockout were most apparent in the injury model, in which the UUO kidneys were bulged and filled with fluid. Kidneys from 3-month-old *Mx1Cre:Survivin*$^{flox/flox}$ mice showed severe gross anatomic kidney defects. Cross-sectional analysis further showed that inactivation of *survivin* at 1 week of age was sufficient to induce kidney cyst formation at 5 weeks of age, although it was not as severe as those with UUO surgery (Figure 2B). Histology analysis using standard hematoxylin and eosin and fluorescent lectin staining confirmed a gross structure abnormality in *Survivin* knockout kidney, especially in the injury model, compared with wild-type age-matched kidneys undergoing the same surgery. Survivin inactivation resulted in a progressively more severe cystic kidney phenotype in older mice.

Survivin Downregulation Exacerbates Aneurysm Formation

The occurrence of aneurysm represents a major risk factor for morbidity and mortality associated with PKD.[15] To examine whether *Survivin* knockout would result in aneurysm, we induced aneurysm formation in endothelium-specific *Survivin* knockout (*PdgfβCre:Survivin*$^{flox/flox}$) mice. These mice were later euthanized to measure the aorta diameter at the site of the aneurysm surgery. Unlike wild-type mice, in which aorta diameter was only slightly enlarged after aneurysm surgery, *Survivin* knockout mice displayed a gross aortic aneurysm similar to that of *PdgfβCre:Pkd1*$^{flox/flox}$, *Pkd2*$^{+/-}$, or *Tg737*$^{Orpk/Orpk}$ mice after aneurysm surgery (Figure 3A). Histological analysis of the cross sections further confirmed a marked arterial enlargement and aneurysm

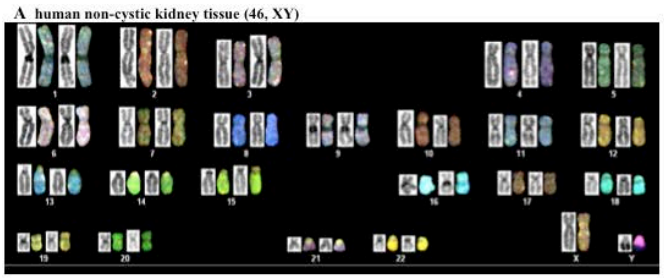

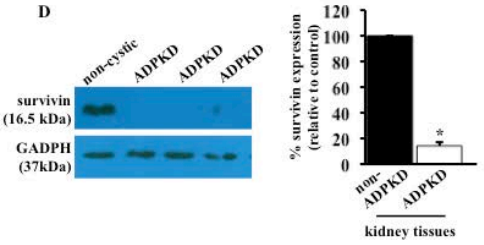

C

kidney samples	normal	tetraploidy	aneuploidy	count (N)	% abnormal
non-ADPKD	34	0	2	36	6
ADPKD	35	12	11	58	40

Figure 1. Autosomal-dominant polycystic kidney disease (ADPKD) renal epithelia are characterized by abnormal ploidy level and survivin downregulation. **A**, Karyotyping was carried out in freshly isolated epithelial cells from non-ADPKD patients to visualize individual chromosomes (noncystic kidney). **B**, Characterization of individual chromosomes from a single renal epithelium isolated from an ADPKD patient indicated tetraploid and abnormal chromosomal composition. **C**, Overall karyotype analysis of individual cells confirmed the presence of abnormal genomic compositions (aneuploidy or polyploidy) in cells from ADPKD patients. **D**, Kidney tissues from ADPKD patients were also used to confirm survivin expression, and GADPH was used as loading control. Bar graph shows relative survivin expression levels. n=3 each for freshly isolated non-ADPKD and ADPKD kidneys.

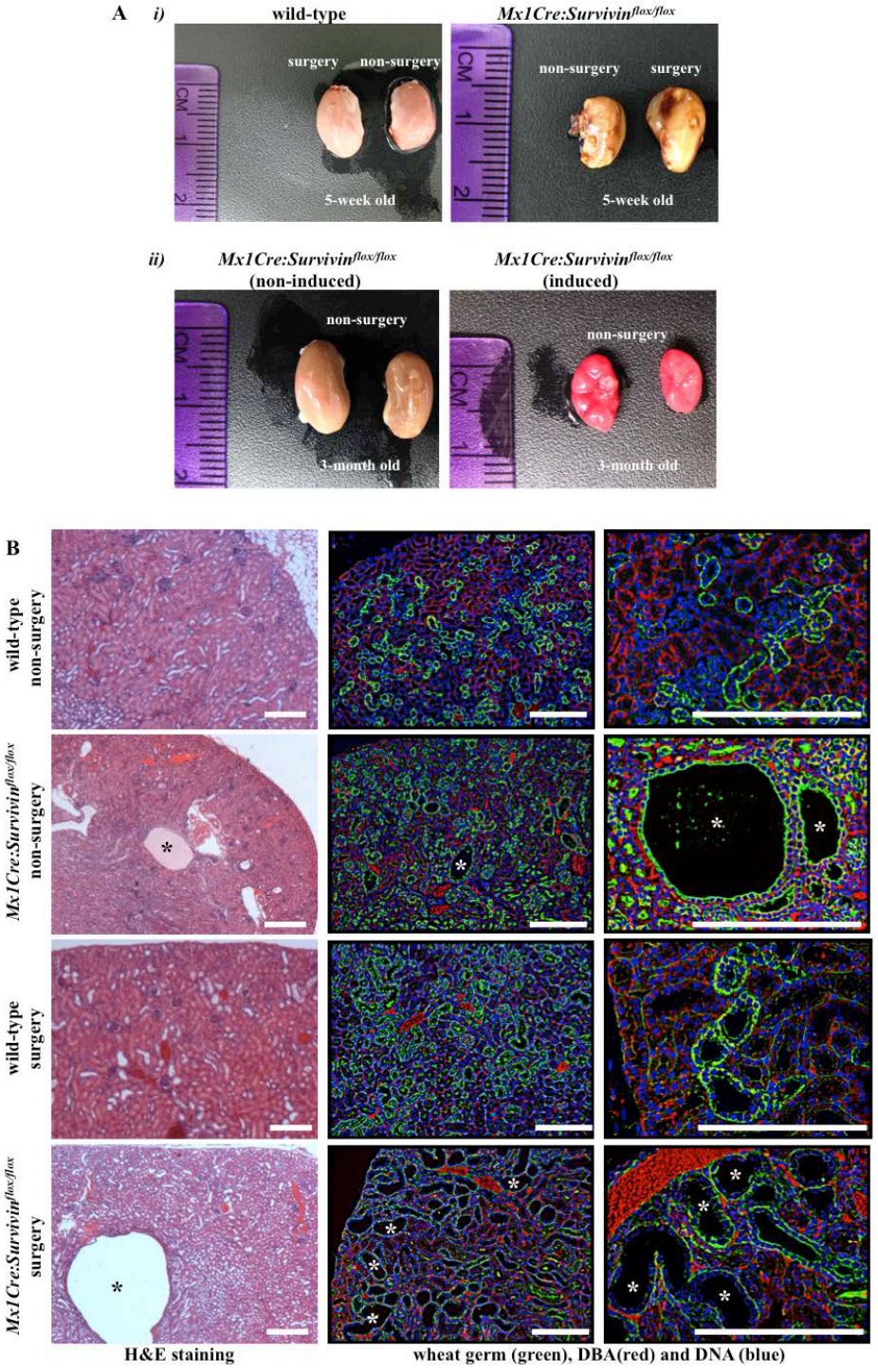

Figure 2. Survivin downregulation is sufficient to induce cystic kidney formation. **A-i**, Unilateral ureteral obstruction (UUO) was performed on either wild-type or *Survivin* knockout (*Mx1Cre:Survivin*$^{flox/flox}$) mice at 1 month of age, and mice were euthanized a week later. **A-ii**, *Mx1Cre:Survivin*$^{flox/flox}$-induced and noninduced littermates were euthanized, and their kidneys were compared 3 months later. Comparison of gross features revealed enlargement in *Survivin* knockout kidneys with an apparent bulged and fluid-filled kidney. **B**, Hematoxylin and eosin (H&E)–stained kidney sections from 5-week-old wild-type and *Mx1Cre:survivin*$^{flox/flox}$ mice with or without UUO surgery are shown. Florescence studies were performed with lectin Dolichos Biflorus Agglutinin (DBA) staining (red) and counterstained with wheat germ agglutinin (green) and DAPI (blue).

formation at the site of surgery from *PdgfβCre:Survivin*$^{flox/flox}$, *PdgfβCre:Pkd1*$^{flox/flox}$, *Pkd2*$^{+/-}$, and *Tg737*$^{Orpk/Orpk}$ mice (Figure 3B). Surprisingly, the *Pkd2*$^{+/-}$ mice also demonstrated a high propensity for aneurysm formation. Our data clearly indicated that similar to *Pkd1*, *Pkd2*, or *Tg737* inactivation, *Survivin* knockout resulted in aneurysm formation (Figure 3C). We next categorized the aneurysm types according to the classification by Daugherty et al.[16] Regardless of the genotypes, the mutant mice consistently showed a more severe grade than the wild-type mice (Figure 3D). Taking these results together, we proposed that vascular and kidney phenotypes of PKD may share a similar cellular mechanism through survivin.

Cellular Mechanism of Cystic and Aneurysm Formation Involves Polyploidy Formation Resulting From Abnormal Cell Division

To examine the mechanism by which survivin downregulation contributes to cystic kidney and vascular aneurysm, we performed live-cell imaging on renal epithelia (Figure 4A). As expected, we observed a symmetrical division in normal epithelial cell (Movie I in the online-only Data Supplement). Although survivin knockdown epithelium committed to enter cell division, severe cytokinesis defect was observed, resulting in failure to exit mitosis properly (Movie II in the online-only Data Supplement). This, in turn, led to polyploidy formation with cytomegaly and multinucleated phenotypes.

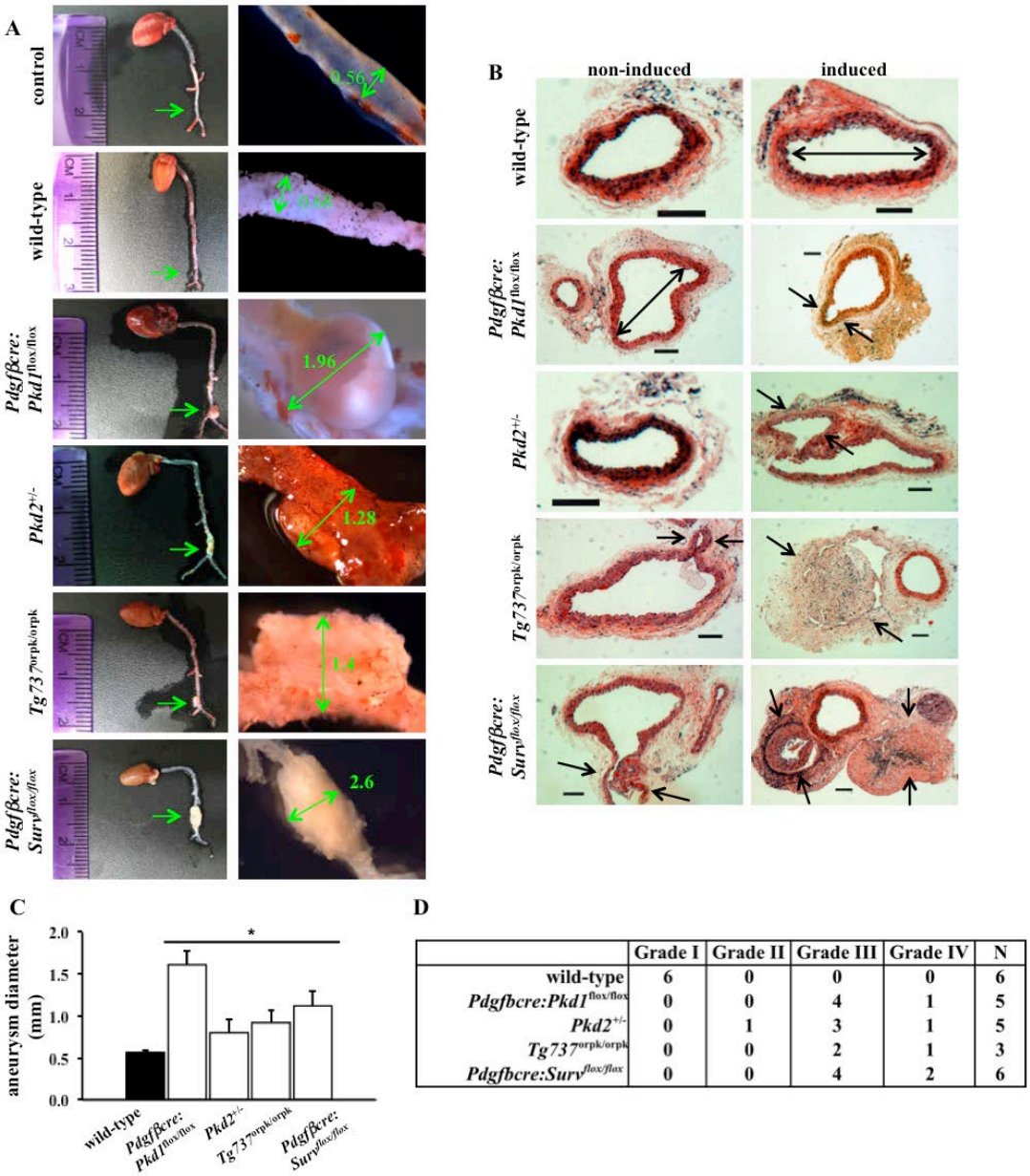

	Grade I	Grade II	Grade III	Grade IV	N
wild-type	6	0	0	0	6
Pdgfbcre:Pkd1$^{flox/flox}$	0	0	4	1	5
Pkd2$^{+/-}$	0	1	3	1	5
Tg737$^{orpk/orpk}$	0	0	2	1	3
Pdgfbcre:Surv$^{flox/flox}$	0	0	4	2	6

Figure 3. Aneurysm formation is an extrarenal phenotype of polycystic kidney disease. **A**, Aneurysm surgery was performed in mice at 1 month of age, and mice were euthanized at 3 months of age. The aortas were isolated and their diameters were measured at the surgical site. Unlike wild-type mice, *Pdgfβcre:Survivin*$^{flox/flox}$ mice showed a severe aneurysm induction to an extent similar to that shown in *Pdgfβcre:Pkd1*$^{flox/flox}$, *Pkd2*$^{+/-}$, and *Tg737*$^{orpk/orpk}$ mice. **B**, Representative cross sections of aortas at the aneurysm surgery site are shown in control wild-type, *Pdgfβcre:Pkd1*$^{flox/flox}$, *Pkd2*$^{+/-}$, *Tg737*$^{orpk/orpk}$, or *Pdgfβcre:Survivin*$^{flox/flox}$ mice with and without aneurysm surgery. Similar to *Pdgfβcre:Pkd1*$^{flox/flox}$, *Pkd2*$^{+/-}$, and *Tg737*$^{orpk/orpk}$ mice, *Pdgfβcre:Surv*$^{flox/flox}$ mice exhibited aneurysm formation and aortic dilation compared with wild-type mice. Arrows point to aneurysm formation, and double-headed arrows point to aorta diameter. n≥3 for each group and genotype. Bar, 200 μm. **C**, Bar graph shows averaged values for aorta diameter in wild-type, *Pdgfβcre:Pkd1*$^{flox/flox}$, *Pkd2*$^{+/-}$, *Tg737*$^{orpk/orpk}$, or *Pdgfβcre:Survivin*$^{flox/flox}$ mice. **D**, The grade of aneurysm is also tabulated.

Similar studies were performed on vascular endothelial cells (Figure 4B). Likewise, similar observations were obtained in control endothelia (Movie III in the online-only Data Supplement) and survivin knockdown endothelia (Movie IV in the online-only Data Supplement).

Polyploidy Formation Contributes to Abnormal Oriented Cell Division in Cystic Expansion and Aneurysm Formation

Oriented cell division dictates the maintenance of renal tubule diameter during tubular lengthening. Defects in this process will trigger renal tubular enlargement and cyst formation in *Pkd* rodent models.[17,18] We thus examined this possibility in *Survivin* mice. Unlike kidney sections from wild-type mice in which normal cell division orientation was parallel to the axis of kidney tubules, kidney sections from *Survivin* knockout mice (*Mx1Cre:Survivin*$^{flox/flox}$) revealed abnormal cell division and orientation pattern (Figure 5A). Both mitotic misorientation and abnormal cell division were very apparent in the *Survivin* knockout mice, particularly after UUO surgery. Abnormal cell divisions include enlarged nucleus, multinucleated cells, or asymmetrical mitosis. Our data further strengthened the argument that survivin shared a similar

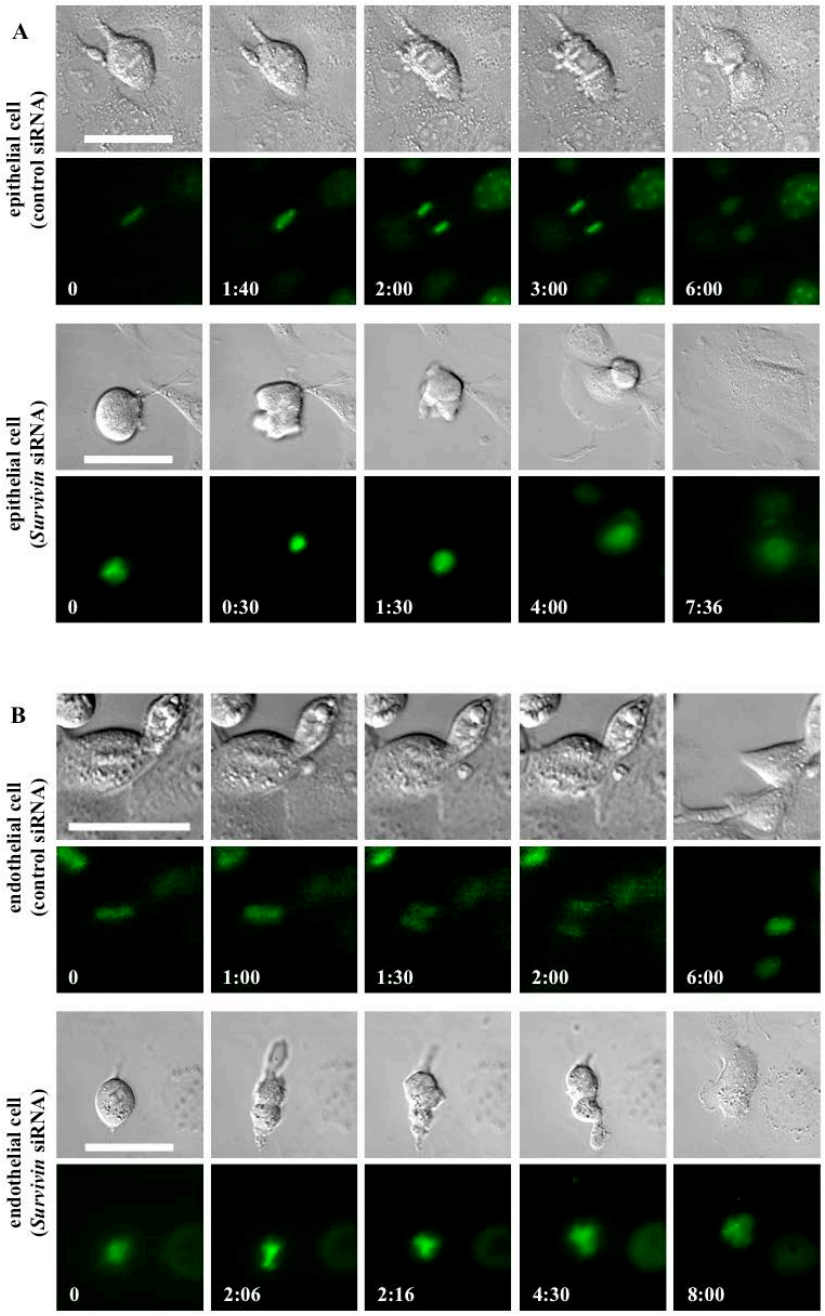

Figure 4. Survivin downregulation is associated with abnormal cytokinesis in primary cells of renal epithelia and vascular endothelial cells. **A**, To obtain the mechanistic insights of cytokinesis defect in renal epithelial cells, live-cell imaging analysis was performed. **B**, A similar study was also done in vascular endothelial cells. Control and survivin knockdown cells were loaded with Hoechst dye to examine nuclear division (**bottom**), whereas differential interference contrast (DIC) images were used to study cytokinesis (**top**). Time stamps indicate hours and minutes as illustrated in the Materials section and Movies I through IV in the online-only Data Supplement. Bar, 50 μm. n≥3 for each group and treatment.

cellular mechanism, as previously reported in polycystic kidney models.[17–19]

To further test our hypothesis that the pathogenesis of aneurysm and cystic kidney shared a common cellular mechanism, we examined for the first time how oriented cell division contributed to aneurysm formation in both *Survivin* and *Pkd* mouse models (Figure 5B). We studied cell division, cell-cell orientation, and division orientation in aortas from wild-type, *PdgfβCre:Pkd1*$^{flox/flox}$, *Pkd2*$^{+/-}$, *Tg737*$^{Orpk/Orpk}$, and *PdgfβCre:Survivin*$^{flox/flox}$ mice. Aorta sections from control wild-type mice displayed normal cell division orientation patterns; however, cell division orientation was slightly perturbed after aneurysm surgery. Similarly, aorta sections from *Pkd2*$^{+/-}$ mice displayed normal cell or cell division orientation, but they showed abnormal cell division after aneurysm surgery. On the other hand, aorta sections from *PdgfβCre:Pkd1*$^{flox/flox}$, *Tg737*$^{Orpk/Orpk}$, and *PdgfβCre:Survivin*$^{flox/flox}$ mice displayed abnormal cell division, cell-cell orientation, and cell division orientation with or without aneurysm surgery.

Primary Cilia Regulate Cell Division Through Survivin Expression

We previously showed that low survivin expression is associated with abnormal mitotic events in endothelial cells with cilia dysfunction.[5] To test our hypothesis that cilia function regulated survivin expression, we examined whether and how flow-induced cilia activation could regulate survivin expression. Wild-type, *Pkd1*$^{-/-}$, and *Tg737*$^{Orpk/Orpk}$ endothelial cells were subjected to fluid shear stress, and survivin expression was analyzed (Figure 6A). The differential expression of survivin between wild-type and cilia mutant cells was most obvious in the presence of fluid shear stress. Survivin expression increased after fluid flow in wild-type but not in cilia mutant cells. However, expression of aurora-A kinase was

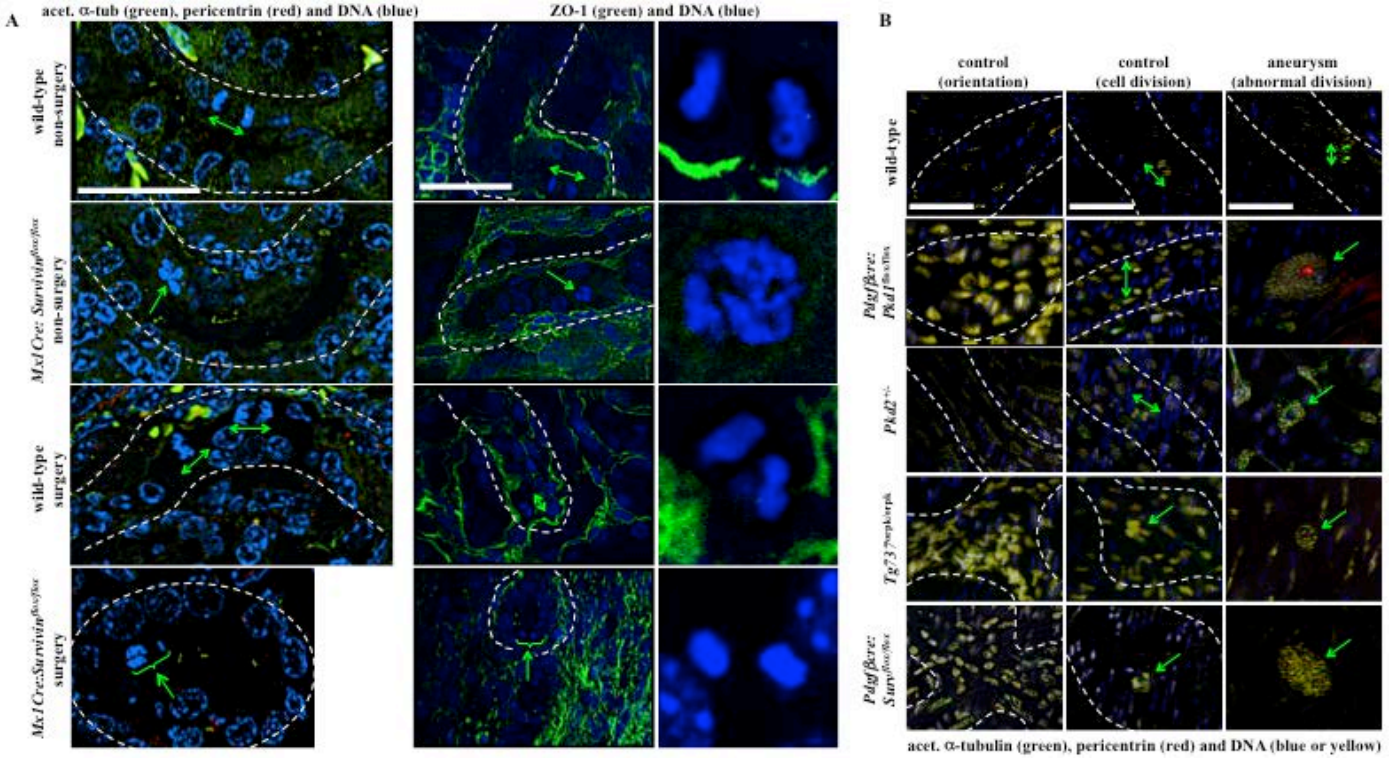

Figure 5. Abnormal cellular division orientation is associated with renal cystic and vascular aneurysm phenotypes. **A**, Kidney tubular sections from both *Mx1Cre:survivin*$^{flox/flox}$ mice, with or without unilateral ureteral obstruction surgery, showed abnormal cell division and division orientation with respect to the axis of the kidney tubule. ZO-1 staining was used to indicate renal tubule orientation, and a cell undergoing division within the region is further enlarged. **B**, Longitudinal abdominal aortic sections in nonsurgery (control) and aneurysm-induced (surgery) models were studied to analyze endothelial orientation and cell division. Nucleus from smooth muscle cells is shown in blue; the nucleus of a single intimal layer of endothelial tissue is pseudocolored in yellow. Abnormal randomized cell orientation is clearly visible. In all figures, division orientation relative to tubule/artery axis is shown in green double-headed arrows, and abnormal cell division is indicated by green arrows. n≥3 for each group and genotype. n≥100 for distribution of spindle orientation angle for each genotype and each treatment. Bar, 40 μm. Acet. α-tub indicates acetylated α-tubulin.

maintained at the same levels in all cells after fluid flow, indicating the specificity of flow-induced survivin expression. More surprising is that fluid flow induced survivin localization to primary cilia only in wild-type cells (Figure 6B). An increase in survivin expression and localization to cilia were not observed in cilia mutant cells in response to fluid shear stress, indicating that fluid flow was acting directly on cilia to induce survivin expression.

We next treated wild-type, *Pkd1*$^{-/-}$, and *Tg737*$^{Orpk/Orpk}$ cells with survivin or aurora-A inhibitors. At resting state (Figure 6C-i), such an inhibition resulted in centrosome overamplification with multiple stubby cilia formation. In dividing cells (Figure 6c-ii), inhibiting survivin or aurora-A induced mitotic arrest with profound defects in the bipolar spindle formation. Defects in resting and dividing cells were observed in wild-type cells, and they became more widespread in cilia mutant cells. Taken together, our data indicated that survivin expression was regulated by flow-induced cilia activation and that both survivin and aurora-A played critical roles in centrosomal number and cell division regulation.

Survivin Expression Is Regulated by PKC, Akt, and Nuclear Factor-κB

We previously demonstrated that PKC and Akt are downstream messengers of primary cilia.[5] Here, we asked whether cilia-induced survivin expression was also mediated by PKC or Akt. To assess whether Akt was downstream of PKC, we treated wild-type and cilia mutant cells with PKC inhibitor or PKC activator (Figure 7A). Expression of phosphorylated Akt (p-Akt) was significantly downregulated in all groups treated with PKC inhibitor compared with control nontreated groups. Moreover, p-Akt was significantly increased in cells treated with PKC activator. Consistent with a previous report,[20] our data support that Akt was downstream of PKC. We next analyzed whether Akt expression was dependent on cilia function (Figure 7B). Cilia activation by fluid flow caused a significant increase in p-Akt level in wild-type but not in cilia mutant cells. Moreover, this increase in p-Akt expression by fluid shear stress was repressed in wild-type cells treated with PKC inhibitor, indicating that Akt activation was dependent on cilia function and required PKC activity. In mutant cells, p-Akt expression was consistently and significantly depressed by PKC inhibitor. On the other hand, changes in aurora-A expression were not consistently observed in all groups after fluid shear stress or PKC inhibitor. We next examined whether aurora-A would regulate p-Akt, Akt, or survivin expression levels (Figure 7C). Our data demonstrated that although inhibiting aurora-A caused no apparent changes in p-Akt or Akt expression, the survivin level was slightly but not significantly altered. This suggested that aurora-A was neither regulated by fluid flow nor upstream of Akt.

It has been reported that Akt can regulate nuclear factor-κB (NF-κB), which is known to regulate survivin expression.[21,22] To investigate this possibility in our system, we studied both

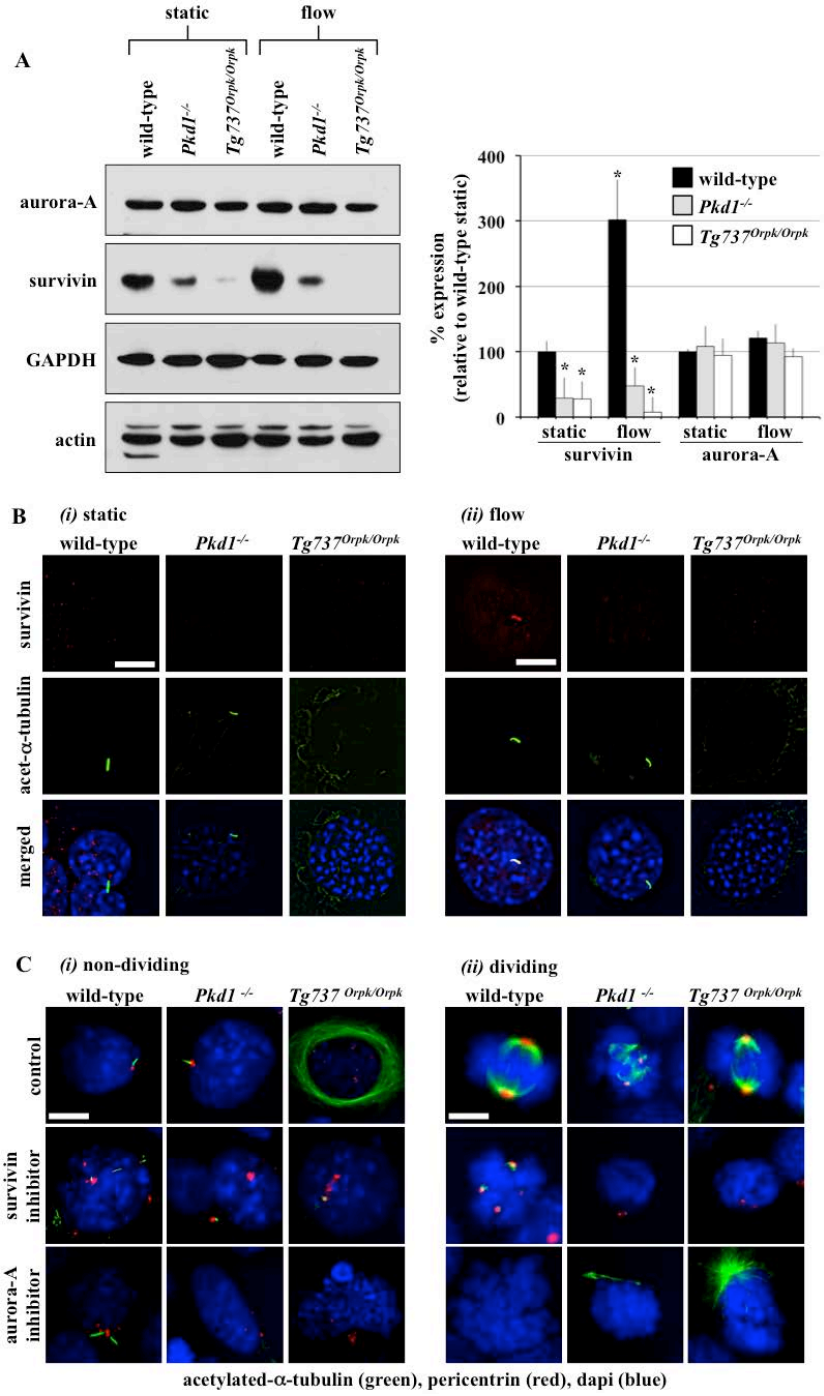

Figure 6. Cilia regulate cell division through survivin expression. **A**, Western blot analysis was used to study survivin and aurora-A expressions in wild-type and cilia mutant cells (*Pkd1*$^{-/-}$ and *Tg737*$^{Orpk/Orpk}$) in the presence or absence of fluid shear stress. GAPDH and actin were used as loading controls. Bar graph represents averaged survivin and aurora-A expressions. **B**, Acetylated α-tubulin (acet. α-tub) was used as a ciliary marker to indicate ciliary expression and localization of survivin in response to fluid shear in wild-type but not mutant cells. **C**, Cells treated with survivin or aurora-A inhibitors are characterized by multiple centrosomes, abnormal mitotic spindle, and mitotic arrest during cell division. Cells were stained with acetylated α-tubulin (green) and pericentrin (red) and captured at resting **(i)** and dividing **(ii)** stages of the cell cycle. Bar, 10 μm. n=3 for each cell type and treatment. Statistics was performed by comparing individual group with their corresponding wild-type static control groups.

NF-κB and phosphorylated NF-κB. We further inhibited aurora-A in the presence of fluid flow to confirm our earlier results and to study the relationship between aurora-A and NF-κB (Figure 7D). Our study corroborated our previous results that flow induces Akt phosphorylation[5] and that this induction was not affected by aurora-A inhibition. Consistent with our earlier studies, survivin expression was increased by flow, although this increase could be repressed by aurora-A inhibitor in the wild-type cells. More important, both NF-κB and phosphorylated NF-κB expressions were significantly increased in the presence of fluid flow in wild-type cells. No obvious changes of NF-κB and phosphorylated NF-κB expressions in response to fluid flow were observed in cilia mutant cells, although the basal level of NF-κB in the mutant cells was higher than in wild-type cells.

We thus far used various pharmacological agents to examine potential signaling pathways, amid some might have nonspecific or off-target effects. Therefore, we next used siRNA knockdown approaches to verify our proposed pathway (Figure 7E). Knockdown of PKC or Akt resulted in downregulation of p-Akt, aurora-A, and survivin expression. Aurora-A knockdown resulted in a decreased expression of aurora-A and survivin, whereas survivin knockdown showed a decrease in survivin expression only. The expression level of a common cell cycle marker, cyclin-B1, did not change after the siRNA studies, confirming that these knockdowns did not affect cell cycle and proliferation status in our cells. Taking these results together, we propose that the cilia-PKC–Akt–NF-κB pathway was involved in survivin expression and cell division regulation.

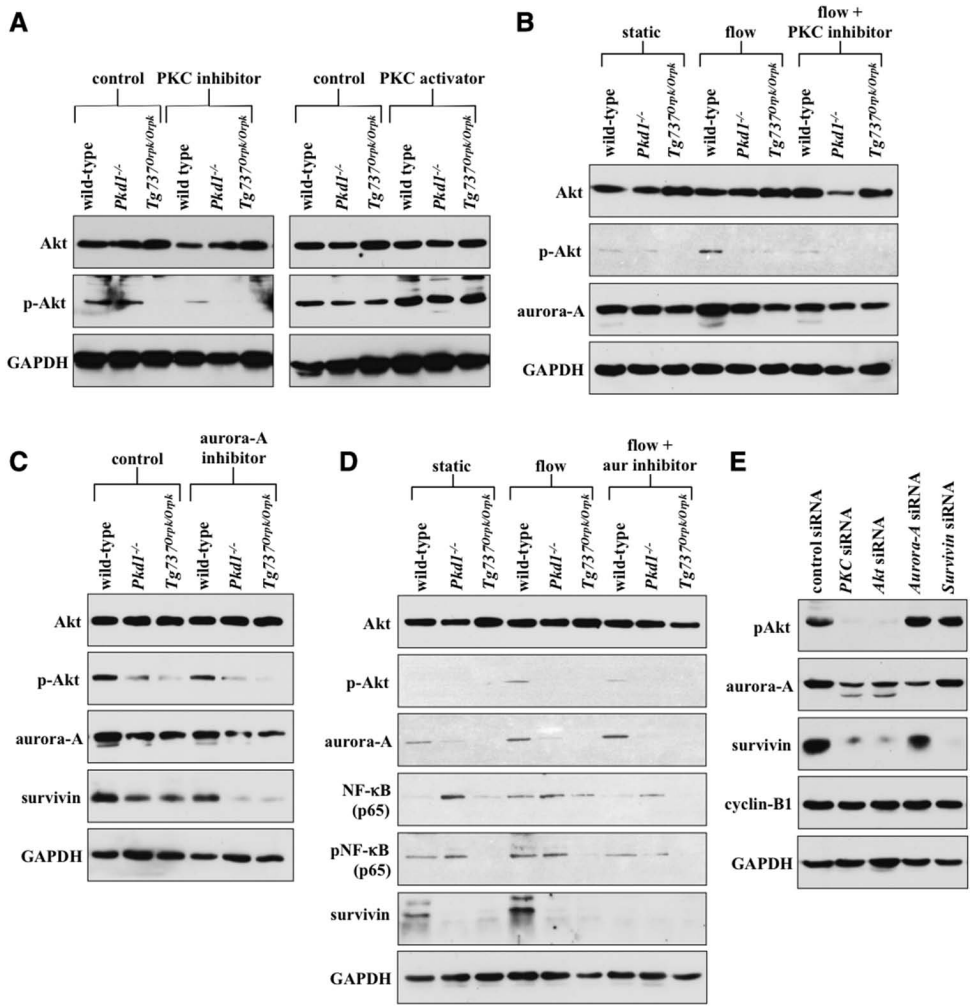

Figure 7. Protein kinase C (PKC)/Akt/nuclear factor-κB (NF-κB) signaling pathway regulates flow-induced survivin expression and cell division. **A**, After wild-type and cilia mutant (*Pkd1*$^{-/-}$ and *Tg737*$^{Orpk/Orpk}$) cells were treated with PKC inhibitor or activator, both Akt and phosphorylated (p-) Akt were analyzed. When treated with PKC inhibitor, all cell lines showed downregulation of p-Akt, whereas PKC activator treatment showed an increase in p-Akt compared with nontreated control cells. **B**, The effect of fluid flow on Akt and aurora-A expression was analyzed in the presence or absence of PKC inhibitor. When subjected to fluid shear, p-Akt expression was upregulated only in wild-type cells. Although p-Akt expression returned to basal levels after treatment with PKC inhibitor and fluid shear stress in wild-type cells, it stayed repressed in mutant cells. **C**, Treatment with aurora-A inhibitor resulted in a decrease in p-Akt, aurora-A, and survivin expression; however, these decreases were not significant compared with the control, nontreated group. **D**, Although the total Akt level was not changed, fluid shear stress significantly induced the expression of p-Akt in wild-type but not in mutant cells. Aurora-A expression was increased after fluid shear stress in wild-type cells; however, this increase was not significant compared with control. Both NF-κB and phosphorylated NF-κB (pNF-κB) expressions were increased after fluid shear stress only in wild-type cells, whereas mutant cells maintained a high basal level of NF-κB compared with static wild-type cells. Survivin expression was increased after shear stress in wild-type cells. **E**, Western blot analyses were conducted to confirm the signaling mechanism involving survivin expression by siRNA-mediated knockdown of PKC, Akt, aurora-A, or survivin. To further confirm the involvement of these signaling molecules in centrosome number and cell division abnormality, immunofluorescence and flow cytometry analyses are presented in the Materials section in the online-only Data Supplement, together with the statistics.

Re-Expression of Survivin Rescues PKD Phenotypes

Because *Survivin* knockout results in PKD phenotypes, it is expected that re-expression of survivin to normal levels should alleviate those phenotypes. To test this hypothesis, we used a zebrafish model for our in vivo studies. It has previously been reported that morpholino (*MO*)-induced depletion of *pkd2* causes profound developmental abnormalities, including cystic kidneys, curly tails, and pericardiac edema in zebrafish embryos.[11] We determined whether we could rescue the *Pkd2* morphants from these phenotypes by coinjecting mRNAs encoding the open reading frame of *survivin*. Because VEGF is known to induce survivin expression through the Akt–NF-κB pathway,[5,21] we also tested whether modulating this pathway by coinjecting VEGF would rescue PKD phenotypes. Our studies showed that coinjection of *survivin* mRNA or VEGF in morpholino knockdown of *pkd2* rescued the curly tail and cystic kidney phenotypes (Figure 8A). Overall data analysis showed that the rescue by *survivin* mRNA or VEGF was more apparent in younger (28 or 48 hours after fertilization) than older (72 hours after fertilization) fish. This was likely attributable to a decrease in the effectiveness or stability of injected survivin mRNA or VEGF as the fish developed to older stages. To examine whether *pkd2MO* zebrafish was associated with survivin downregulation as seen in the human

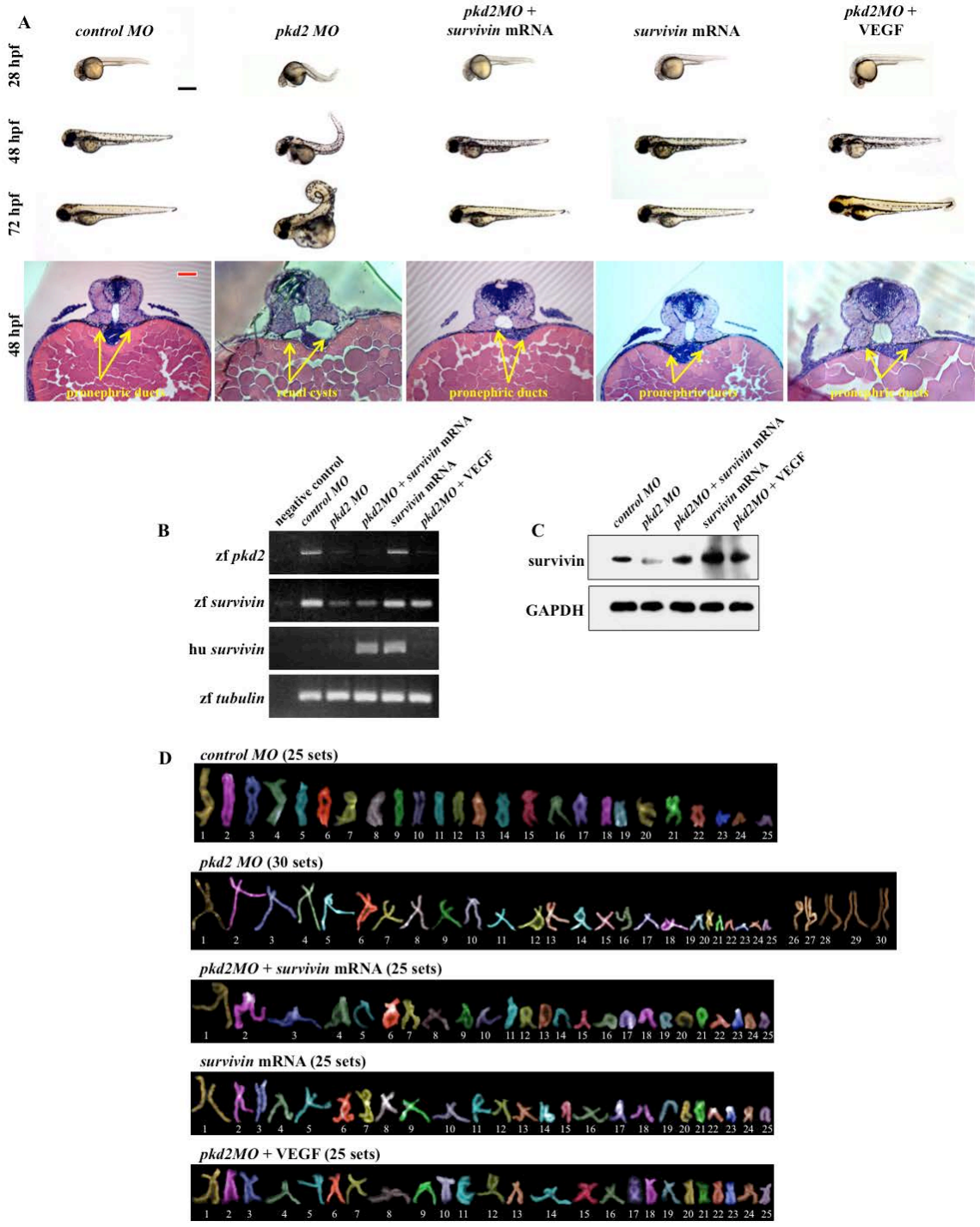

Figure 8. Survivin overexpression rescued polycystic kidney disease phenotypes in zebrafish. **A**, Zebrafish embryos were scored for phenotypic observations at different developmental stages. Shown here are representative images of zebrafish at 24, 48, and 72 hours postfertilization (hpf) injected with control morpholino (*MO)*, *pkd2 MO*, *pkd2 MO* plus *survivin* mRNA, *survivin* mRNA alone, or *pkd2 MO* plus vascular endothelial growth factor (VEGF). Abnormal phenotypes associated with *pkd2 MO* injections such as curly tail and renal cyst were rescued by *survivin* mRNA or VEGF injection into zebrafish embryos. Representative images of 48-hpf zebrafish sections are shown. The sections were stained with hematoxylin and eosin (**bottom**); and arrows point to pronephric structures. **B**, Reverse transcription–polymerase chain reaction (RT-PCR) was performed to examine zebrafish (zf) and human (hu) transcript levels for *survivin* and to confirm *pkd2* knockdown. Human survivin was introduced through mRNA injection. α-Tubulin was used as a loading control. **C**, Expression levels of survivin were analyzed in all the groups in which zebrafish and human survivin can be recognized by the same antibody. **D**, Analyses of individual chromosomes were performed in all groups of fish embryos to study chromosomal number. Black bar, 500 μm; red bar, 50 μm. All quantification and statistical analyses on Western blot, RT-PCR, and polyploidy level are presented in the Materials section in the online-only Data Supplement.

PKD and mouse models, we studied the levels of survivin transcript (Figure 8B) and protein (Figure 8C). The endogenous zebrafish *Pkd2* transcript levels were decreased in *pkd2MO*-, *pkd2MO* plus *survivin* mRNA–, or *pkd2MO* plus VEGF–injected embryos compared with *controlMO* fish. Injection of *survivin* mRNA alone did not alter the zebrafish

pkd2 transcript. Furthermore, the endogenous zebrafish *survivin* transcript levels were significantly decreased in the presence of *pkd2MO*, but this could be rescued by VEGF. Our data suggested that the PKD phenotypic rescue in *pkd2MO* plus VEGF–injected embryos was achieved via induction of endogenous zebrafish *survivin*, unlike in *pkd2MO* plus *survivin* mRNA–injected embryos, in which rescue depended on exogenous human *survivin*. Survivin protein was then quantified using an antibody that recognizes both human and zebrafish forms. Our analysis confirmed the decrease of survivin expression in *pkd2MO* fish and indicated that survivin expression could be rescued by human *survivin* mRNA or VEGF injection, leading to PKD phenotypic rescue.

To study how survivin rescued the PKD phenotypes, we investigated whether a molecular mechanism similar to human PKD and mouse models might involve abnormal polyploidy formation in zebrafish. Analysis of individual chromosomes confirmed a significant increase in polyploidy formation from cells derived from *pkd2MO* fish compared with those derived from *controlMO* fish (Figure 8D). This polyploidy increase could be partially rescued after coinjection with *survivin* mRNA. Overall, our data suggested that survivin played an important role in regulating ploidy, a common cellular contributor to PKD phenotypes.

Discussion

Our studies show that abnormal function of mechanosensory cilia leads to survivin downregulation, which is associated with abnormal ploidy formation and contributes to cystic kidney and vascular aneurysm phenotypes. We show for the first time that *Survivin* conditional knockout in the kidney or vascular tissues is associated with cyst or aneurysm formation, respectively. At least in the zebrafish model, re-expression of survivin can partially rescue PKD phenotypes. Overall, our studies demonstrate that primary cilia control renal and vascular architectures through survivin expression and symmetrical cell division along the longitudinal axis of the tissues.

Data from our PKD patients are supported strongly by the mouse and zebrafish studies, indicating that survivin downregulation triggers polyploidy formation, the predominant phenotype observed throughout our studies. In our controls, especially in human samples, some polyploidy was detected. This is most likely attributable to a physiological aging process characterized by cellular senescence.[23] A subpopulation of our precystic cells exhibited 8 N DNA content, suggesting that consecutive rounds of DNA replication without proper cell division are still possible in cells with a low survivin expression. This is consistent with the report that *survivin* deletion causes an overall decrease in cell number at the expense of DNA accumulation.[24] We further propose that polyploidy could potentially be used as an early marker in PKD. It is noteworthy that the sensitivity of the karyotyping technique is far superior to that of flow cytometry in single-cell analyses.[10] Thus, changes in chromosome number can easily be identified with absolute certainty in PKD patients before end-stage renal failure.

To ensure the clinical relevance of our findings in age- and sex-matched patients, we used noncystic and PKD human epithelial cell lines (Figure I in the online-only Data Supplement). We also used *Pkd2* and *Tg737* mouse models to verify our clinical data. Our mouse data supported the idea that polyploidy formation precedes cystic expansion and contributes to vascular aneurysm. As in human cell lines, all kidneys from *Pkd* mouse model samples were characterized by polyploidy and had a significant downregulation in survivin expression.

Given the evidence that kidney injury will trigger tubular epithelial cell proliferation,[25] in which survivin is required, it is not surprising that *Mx1Cre:Survivin*$^{flox/flox}$ mice exhibited more severe cystic kidneys in UUO-induced injury compared with their nonsurgical counterparts. In *Mx1Cre:Survivin*$^{flox/flox}$ mice with no surgery, the cystic kidney phenotype progressively became more severe with aging. Similar to *Pkd* mouse models, inactivation of vascular *Survivin* exhibited no apparent or consistent phenotype in 1-month-old adult mice. Especially during injury, however, survivin downregulation genetically or pharmacologically was directly linked to cystic kidney formation (Figure II in the online-only Data Supplement). To facilitate and accelerate vascular phenotype, we used a $CaCl_2$ aneurysm induction model. Not only in *survivin* but also in other *Pkd* mouse models, abnormal cell division or cilia function is sufficient to exacerbate the aneurysm phenotype and atherosclerotic plaques after the surgery. Homozygous *Survivin* knockout mice are also characterized by multinucleation, polyploidy, and apoptosis,[9] which are also seen in our renal epithelia and vascular endothelia of *Survivin*, *Pkd1,* and *Tg737*.

Downregulation of survivin was associated with apoptosis (Figure III in the online-only Data Supplement). More important, when blood pressure was monitored in our mutant mice, *Survivin* knockout mice surprisingly did not show an elevated blood pressure. This was consistent with the general understanding that hypertension itself does not account for aneurysm development.[26] Supporting this view, patients with PKD have a significantly greater chance of developing aneurysm than the general population with hypertension.[27]

Oriented cell division is involved in a variety of processes that contribute to organ shape and morphogenesis and are involved in coordinated cell division, differentiation, and spatial distribution. Elongation of the kidney tubule is also associated with oriented cell division, which when perturbed would result in cystic formation.[17–19] We show here not only that oriented cell division was perturbed in our *survivin*-inactivated renal tubules but also that the asymmetrical cell division phenotype was evident in dividing tubular cells. The mechanism of disturbed cell division and mitotic orientation was also confirmed for the first time in the arteries of *Survivin*, *Pkd1*, *Pkd2*, and *Tg737* mice. These mice show distorted cell division and mitotic spindle orientation, even before the aneurysm is formed, as also evidence from our studies on mitotic stress test and ploidy level in survivin knockdown epithelial and endothelial cells (Figures IV and V in the online-only Data Supplement). Overall, our comprehensive studies suggest that survivin downregulation is involved in the control of cell division, polypoidy, and asymmetrical division orientation. Furthermore, the control of cell division orientation defined a common mechanism for both cystic expansion and aneurysm formation in the *Pkd* and *survivin* mouse models.

Survivin, together with aurora-A kinase, regulates several distinct mitotic events such as the formation of mitotic spindle and cytokinetic ring.[8] We examined aurora-A kinase in our study because aurora-A has been shown to be localized to the basal body of primary cilia[28] and expressed abnormally in the cyst-lining renal epithelia.[29] Generally, neither survivin nor aurora-A was mislocalized in the mutant cells at different stages of cell division (Figure VI in the online-only Data Supplement). Our present data also suggest that aurora-A expression is not regulated by cilia activation through fluid flow. Nonetheless, our study reinforces the localization of aurora-A to the centriole in the resting stage and to the centrosome and midbody during cell division. More important, we demonstrated for the first time that inhibiting aurora-A function or expression would result in defects in cell division, ploidy, centrosomal amplification, cytokinesis, and mitotic spindle formation, all of which were phenotypes associated with survivin downregulation. This suggests that although aurora-A may not be part of the cilia-survivin pathway, aurora-A and survivin may function as molecular partners, reflecting their common roles in the contraction of the cytokinetic ring in regulating cell division (Figure VII in the online-only Data Supplement).

Not only is survivin expression increased after cilia activation, but our study also shows for the first time that its subcellular localization is differentially regulated from centriole to primary cilia after fluid shear stress. These localizations may reflect a novel survivin function in nondividing cells and may contribute to a larger pathological spectrum other than cancer or PKD. Moreover, our immunofluorescence analysis reveals the localization pattern of survivin during mitotic division, specifically during cytokinesis, reflecting its role in cytokinesis. This is also supported by live imaging studies in which survivin knockdown causes severe cytokinesis defects, resulting in cytomegaly and polyploidy phenotypes in both renal epithelia and vascular endothelia (see the movies in the online-only Data Supplement). Despite the finding that survivin expression was dysregulated in the cilia mutant cells, it is worth mentioning that survivin localization was not perturbed during cell division. To further decipher the signaling mechanisms between cilia and survivin expression, we examined the cilia–PKC–Akt–NF-κB–survivin/aurora-A pathway.

In an attempt to elucidate the physiological relevance of survivin downregulation in cystic kidney and vascular phenotypes in PKD, we used a zebrafish model to study the roles of survivin expression. Four novel insights are provided by these studies. First, *pkd2* knockdown is associated with survivin downregulation in zebrafish, which confirms our hypothesis that survivin expression is regulated by cilia function. Second, the rescue of PKD phenotypes associated with *pkd2* knockdown by re-expression survivin provides further evidence for the importance of survivin roles in PKD. Third, VEGF is an attractive modulator to induce survivin expression in *pkd2* knockdown fish. Fourth, *pkd2* knockdown contributes to polyploidy, a common mechanism representing PKD phenotypes as also seen in PKD patients and mouse models (Figure VIII in the online-only Data Supplement).

Conclusions

Our studies provide a novel aspect of the mechanism of pathogeneses of cystic kidney and aneurysm formation in PKD. Our present study shows for the first time that these phenotypes are contributed mainly by abnormal cilia function, resulting in dysregulation of survivin expression. Abnormal survivin expression further causes abnormal cytokinesis, which results in cell polyploidy, multimitotic spindle formation, and aberrant cell division orientation. The asymmetrical cell division, together with abnormal planar cell polarity, contributes to the expansion of tissue architecture, resulting in the formation of cystic kidney and vascular aneurysm. All in all, data from this study suggest that improving survivin expression could be a promising therapeutic target for kidney and vascular complications associated with PKD. Overall, our current working model would be as follows: primary cilia→PKC→Akt→NF-κB→survivin/aurora-A→cytokinesis→polyploidy→asymmetrical cell division/planar cell polarity→cystic kidney and vascular aneurysm (architecture expansion).

Acknowledgments

We thank Charisse Montgomery and Maki Takahashi for their editing services and technical support.

Source of Funding

This work was supported by awards from the National Institutes of Health (DK080640).

Disclosures

None.

References

1. AbouAlaiwi WA, Takahashi M, Mell BR, Jones TJ, Ratnam S, Kolb RJ, Nauli SM. Ciliary polycystin-2 is a mechanosensitive calcium channel involved in nitric oxide signaling cascades. *Circ Res*. 2009;104:860–869.
2. Nauli SM, Alenghat FJ, Luo Y, Williams E, Vassilev P, Li X, Elia AE, Lu W, Brown EM, Quinn SJ, Ingber DE, Zhou J. Polycystins 1 and 2 mediate mechanosensation in the primary cilium of kidney cells. *Nat Genet*. 2003;33:129–137.
3. Nauli SM, Kawanabe Y, Kaminski JJ, Pearce WJ, Ingber DE, Zhou J. Endothelial cilia are fluid shear sensors that regulate calcium signaling and nitric oxide production through polycystin-1. *Circulation*. 2008;117:1161–1171.
4. Xu C, Shmukler BE, Nishimura K, Kaczmarek E, Rossetti S, Harris PC, Wandinger-Ness A, Bacallao RL, Alper SL. Attenuated, flow-induced ATP release contributes to absence of flow-sensitive, purinergic Ca_i^{2+} signaling in human ADPKD cyst epithelial cells. *Am J Physiol Renal Physiol*. 2009;296:F1464–F1476.
5. AbouAlaiwi WA, Ratnam S, Booth RL, Shah JV, Nauli SM. Endothelial cells from humans and mice with polycystic kidney disease are characterized by polyploidy and chromosome segregation defects through survivin down-regulation. *Hum Mol Genet*. 2011;20:354–367.
6. Battini L, Macip S, Fedorova E, Dikman S, Somlo S, Montagna C, Gusella GL. Loss of polycystin-1 causes centrosome amplification and genomic instability. *Hum Mol Genet*. 2008;17:2819–2833.
7. Burtey S, Riera M, Ribe E, Pennenkamp P, Rance R, Luciani J, Dworniczak B, Mattei MG, Fontés M. Centrosome overduplication and mitotic instability in PKD2 transgenic lines. *Cell Biol Int*. 2008;32:1193–1198.
8. Terada Y. Role of chromosomal passenger complex in chromosome segregation and cytokinesis. *Cell Struct Funct*. 2001;26:653–657.
9. Uren AG, Wong L, Pakusch M, Fowler KJ, Burrows FJ, Vaux DL, Choo KH. Survivin and the inner centromere protein INCENP show similar cell-cycle localization and gene knockout phenotype. *Curr Biol*. 2000;10:1319–1328.
10. AbouAlaiwi WA, Rodriguez I, Nauli SM. Spectral karyotyping to study chromosome abnormalities in humans and mice with polycystic kidney disease. *J Vis Exp*. 2012;60:pii: 3887.

11. Sun Z, Amsterdam A, Pazour GJ, Cole DG, Miller MS, Hopkins N. A genetic screen in zebrafish identifies cilia genes as a principal cause of cystic kidney. *Development*. 2004;131:4085–4093.
12. Falleni M, Pellegrini C, Marchetti A, Oprandi B, Buttitta F, Barassi F, Santambrogio L, Coggi G, Bosari S. Survivin gene expression in early-stage non-small cell lung cancer. *J Pathol*. 2003;200:620–626.
13. Ko CY, Tsai MY, Tseng WF, Cheng CH, Huang CR, Wu JS, Chung HY, Hsieh CS, Sun CK, Hwang SP, Yuh CH, Huang CJ, Pai TW, Tzou WS, Hu CH. Integration of CNS survival and differentiation by HIF2α. *Cell Death Differ*. 2011;18:1757–1770.
14. Muntean BS, Horvat CM, Behler JH, Aboualaiwi WA, Nauli AM, Williams FE, Nauli SM. A comparative study of embedded and anesthetized zebrafish in vivo on myocardiac calcium oscillation and heart muscle contraction. *Front Pharmacol*. 2010;1:139.
15. Ecder T, Schrier RW. Cardiovascular abnormalities in autosomal-dominant polycystic kidney disease. *Nat Rev Nephrol*. 2009;5:221–228.
16. Daugherty A, Manning MW, Cassis LA. Antagonism of AT2 receptors augments angiotensin II-induced abdominal aortic aneurysms and atherosclerosis. *Br J Pharmacol*. 2001;134:865–870.
17. Fischer E, Legue E, Doyen A, Nato F, Nicolas JF, Torres V, Yaniv M, Pontoglio M. Defective planar cell polarity in polycystic kidney disease. *Nat Genet*. 2006;38:21–23.
18. Patel V, Li L, Cobo-Stark P, Shao X, Somlo S, Lin F, Igarashi P. Acute kidney injury and aberrant planar cell polarity induce cyst formation in mice lacking renal cilia. *Hum Mol Genet*. 2008;17:1578–1590.
19. Delaval B, Bright A, Lawson ND, Doxsey S. The cilia protein IFT88 is required for spindle orientation in mitosis. *Nat Cell Biol*. 2011;13:461–468.
20. Nazarewicz RR, Salazar G, Patrushev N, San Martin A, Hilenski L, Xiong S, Alexander RW. Early endosomal antigen 1 (EEA1) is an obligate scaffold for angiotensin II-induced, PKC-alpha-dependent Akt activation in endosomes. *J Biol Chem*. 2011;286:2886–2895.
21. Li W, Wang H, Kuang CY, Zhu JK, Yu Y, Qin ZX, Liu J, Huang L. An essential role for the Id1/PI3K/Akt/NFkB/survivin signalling pathway in promoting the proliferation of endothelial progenitor cells in vitro. *Mol Cell Biochem*. 2012;363:135–145.
22. Lin J, Guan Z, Wang C, Feng L, Zheng Y, Caicedo E, Bearth E, Peng JR, Gaffney P, Ondrey FG. Inhibitor of differentiation 1 contributes to head and neck squamous cell carcinoma survival via the NF-kappaB/survivin and phosphoinositide 3-kinase/Akt signaling pathways. *Clin Cancer Res*. 2010;16:77–87.
23. Jones MR, Ravid K. Vascular smooth muscle polyploidization as a biomarker for aging and its impact on differential gene expression. *J Biol Chem*. 2004;279:5306–5313.
24. Levkau B, Schäfers M, Wohlschlaeger J, von Wnuck Lipinski K, Keul P, Hermann S, Kawaguchi N, Kirchhof P, Fabritz L, Stypmann J, Stegger L, Flögel U, Schrader J, Fischer JW, Fischer J, Hsieh P, Ou YL, Mehrhof F, Tiemann K, Ghanem A, Matus M, Neumann J, Heusch G, Schmid KW, Conway EM, Baba HA. Survivin determines cardiac function by controlling total cardiomyocyte number. *Circulation*. 2008;117:1583–1593.
25. Yang L, Besschetnova TY, Brooks CR, Shah JV, Bonventre JV. Epithelial cell cycle arrest in G2/M mediates kidney fibrosis after injury. *Nat Med*. 2011;16:535–543, 1 p following 143.
26. Chen J, Kuhlencordt PJ, Astern J, Gyurko R, Huang PL. Hypertension does not account for the accelerated atherosclerosis and development of aneurysms in male apolipoprotein E/endothelial nitric oxide synthase double knockout mice. *Circulation*. 2001;104:2391–2394.
27. Chapman AB, Rubinstein D, Hughes R, Stears JC, Earnest MP, Johnson AM, Gabow PA, Kaehny WD. Intracranial aneurysms in autosomal dominant polycystic kidney disease. *N Engl J Med*. 1992;327:916–920.
28. Plotnikova OV, Nikonova AS, Loskutov YV, Kozyulina PY, Pugacheva EN, Golemis EA. Calmodulin activation of aurora-A kinase (AURKA) is required during ciliary disassembly and in mitosis. *Mol Biol Cell*. 2012;23:2658–2670.
29. Plotnikova OV, Pugacheva EN, Golemis EA. Aurora A kinase activity influences calcium signaling in kidney cells. *J Cell Biol*. 2011;193:1021–1032.

CLINICAL PERSPECTIVE

Autosomal-dominant polycystic kidney disease (ADPKD) is a ciliopathy characterized by the formation of kidney cysts and vascular aneurysms. Surprisingly, these balloon-like structures in the kidney and blood vessel are greatly associated with one another. Although abnormal cilia function in detecting urine flow will result in kidney cyst formation, inability of cilia to sense blood flow can induce vascular aneurysm. The formation of these balloon-like structures is independent from blood pressure but is tightly regulated by survivin expression. During repair resulting from any physiological perturbation or insult, a proper expression level of survivin is required to maintain the overall architectural structure of an organ. ADPKD with abnormal cilia function fails to maintain this architectural structure because of a low survivin expression, which induces asymmetrical cell division. As a result of this random expansion during cell division, an elongated architecture of a nephron or vasculature will no longer be achieved. It is therefore not surprising that it takes a long period of time to form such structural abnormalities as renal cysts and vascular aneurysms. Our studies also raise some questions: Can a similar mechanism also occur in other organs besides renal and vascular systems in ADPKD? In addition, can we use survivin or cell ploidity as a biomarker to indicate disease progression or severity in ADPKD? More specifically, we have used spectral karyotyping, which only requires 1 single cell from our ADPKD patients to confirm their cellular polyploidity throughout our studies.

SUPPLEMENTAL MATERIAL

Survivin-induced abnormal ploidy contributes to cystic kidney and aneurysm formation

Wissam A. AbouAlaiwi, Ph.D.[1*], Brian S. Muntean, B.Sc.[2*], Shobha Ratnam, M.D.[3], Bina Joe, Ph.D.[4], Lijun Liu, M.D.[5], Robert L. Booth, M.D.[6], Ingrid Rodriguez, D.O.[7], Britney S. Herbert, Ph.D.[8], Robert L. Bacallao, M.D.[9], Marcus Fruttiger, Ph.D.[10], Tak W. Mak, Ph.D.[11], Jing Zhou, M.D., Ph.D.[12], Surya M. Nauli, Ph.D.[1,2,3,4]

[*] These authors contribute equally.

[1]Department of Pharmacology, [2]Department of Medicinal and Biological Chemistry, [3]Department of Medicine, [4]Center for Hypertension and Personalized Medicine, [5]Department of Biochemistry and Cancer Biology, [6]Department of Pathology, The University of Toledo, Toledo, Ohio
[7]Department of Emergency and Intensive Care, ProMedica Sponsored Research, Toledo, Ohio
[8]Department of Medicine, [9]Department of Medical and Molecular Genetics, Indiana University School of Medicine, Indianapolis, Indiana
[10]UCL Institute of Ophthalmology, University College London, London, United Kingdom
[11]Ontario Cancer Institute, University Health Network, Toronto, ON, Canada
[12]Department of Medicine, Brigham and Women's Hospital, Boston, Massachusetts

Corresponding author:
Surya M. Nauli, Ph.D.
University of Toledo
Department of Pharmacology; MS 1015
Health Education building; Room 274
3000 Arlington Ave
Toledo, OH 43614

Phone: 419-383-1910
Fax: 419-383-1909
Email: Surya.Nauli@UToledo.Edu

SUPPLEMENTAL METHODS

Human tissues and cell lines

Signed and informed consent to collect disposed human tissues was obtained from the ADPKD (autosomal dominant polycystic kidney disease) and non-ADPKD patients. The protocols for tissue collection were approved by the Department for Human Research Protections of the Biomedical Institutional Review Board of The University of Toledo. Kidney tissues were collected from both ADPKD and non-ADPKD patients undergoing kidney transplant surgery. The non-cystic (male) and cystic (two males and one female) kidneys were obtained randomly from our hospital. Thus, these samples were not age-matched, but they are freshly collected within one hour after kidney removal from each patient. To ensure proper comparisons of human samples in our studies, we also used well-characterized human cell lines isolated from age- and sex-matched normal and PKD renal epithelia. Importantly, the PKD epithelial cells have been characterized to have abnormal cilia function. These cells also contain a marker of proximal nephron origin, which has previously been confirmed to have Q4004X mutation in *Pkd1* gene[1].

Genetic mouse models

All animal studies were approved by The University of Toledo animal care and use committee. We used both traditional and conditional transgenic mouse models in our present studies. We have previously obtained traditional transgenic *Pkd*-mouse models $Pkd2^{+/-}$ and $Tg737^{Orpk/Orpk}$ from Drs. Somlo[2] and Yoder[3], respectively. We used $survivin^{flox/flox}$ and $Pkd1^{flox/flox}$ conditional mouse models that were previously generated in our laboratories[4, 5]. To generate kidney-specific knockout, we used *Mx1Cre* mice previously confirmed with a *ROSA* model[5]. Briefly, one-week

old pups were injected intra-peritoneally with 62.5 μg of 50 μL polyinosinic:polycytidylic ribonuceic acid (pI:pC) every day for five consecutive days. In some cases, mice were subjected to renal injury at one-month old. Mice were sacrificed at either five-weeks or three-months of age, and their kidney morphologies were analyzed. To generate vascular-specific knockout, we used *PdgfβCre* mice previously confirmed with a *ROSA* model[6]. One-week old pups were injected intra-peritoneally with 250 μg of 50 μL tamoxifen every day for five consecutive days. In some cases, mice were subjected to vascular surgery at two-months old. Mice were sacrificed at three-months old, and their vascular morphologies were analyzed.

UUO and aneurysm inductions

Mouse health was confirmed before and after each surgical procedure. During the surgery, a mask connected to isoflurane regulator was placed over the nose and mouth of the mouse. 3-5% isoflurane was used to induce anesthetics followed by 1-3% isoflurane depending on the response to toe pinching and eye reflex. After shaving the hair around the incision site, skin was scrubbed with a betadine surgical scrub in circular motion from center out followed by 70% isopropyl alcohol. After the procedure was completed, the incision site was closed in a single layer using 4-0 silk suture. The skin was then closed using surgical staples (Clay Adams Autoclips). Mouse was monitored every 15 minutes until awake, followed by daily for 4 days post surgery. Only if the mouse was in pain, buprenorphine at 2.5/kg SQ twice a day was administered. Pain was determined by weight loss, lack of activity and failure to eat or drink. Penicillin G Procaine at 40,000 units/kg IM once a day was given if an infection was suspected. One sign of an infection would be discharge around the incision site.

To induce an experimental cystic model, unilateral ureteral obstruction (UUO) was generated by tying a 6-0 silk suture against a 28G needle in one-month old mice. After removal of the needle, a narrowing of total ureter diameter was achieved. The incision was sealed using a 4-0 silk suture followed by application of surgical staples to close the layer of skin. The mice were sacrificed one week later. To induce an experimental aneurysm model, sterile cotton gauze containing saline (control) or 0.25 M calcium chloride (aneurysm induction) was placed directly on the abdominal aorta for 10 minutes in two-month-old mice. Mice were euthanized at three-months old, at which time the heart and aorta were harvested, photographed, sectioned, and H&E stained to measure the diameter of the aneurysm lesions.

In both renal and vascular studies, we used respective UUO and $CaCl_2$ as models to facilitate and accelerate renal cyst and vascular aneurysm formation. These types of surgery models have been widely used to study kidney[7] and vascular[8] phenotypes. The advantages of such models include a rapid assessment of transgenic rodent models and provide a more precise location of injury, especially for mild aneurysm, which is very hard to spot within the vascular beds. In addition, these models are also characterized by an increased rate of cellular proliferation in kidney repair[7] and neovascularization[8]. This, in turn, will facilitate studying planar cell polarity, especially in non-PKD tissue. Consistent with this idea, it has been shown that cyst formation requires increased rates of cell proliferation[9], in which survivin is required. Although such operations may be less ideal in regard to mechanism and pathology comparison, we have thus collected data from zebrafish and PKD patients to further support our hypothesis. Of note is that increased cell proliferation is a major requirement of phenotypic development in human ADPKD kidney[10] and vascular endothelia[11].

Blood pressure measurement

Systolic and Diastolic blood pressure were monitored by non-invasive blood pressure system - tail cuff method with the aid of a computerized system (CODA system, Kent Scientific, Connecticut, USA). Measurements were performed at the baseline 3-times per week for 2 weeks after previous 3 days of training for each mouse. On each day of blood pressure measurement, 2 sets of 18 measurements were obtained including three measurements of training or acclimation. The measurements were averaged for each mouse with at least three mice for each genotype. All animals were tested by an investigator blinded to the genotypes of the animals. The data from the tail cuff method was also verified with limited studies with a more invasive, surgically implanted telemetry probe (data not shown).

Cell culture

Both primary cultures and cell lines were used in the present studies. The use and isolation of mouse primary tubular cells from distal collecting tubules have been described previously in detail[12]. For cell lines, we used previously generated endothelial cells from embryonic aortas. Various endothelial markers have been confirmed in these cells[13, 14]. More importantly, the mutant cell lines did not respond to fluid-shear stress, a characteristic of *PKD* cells with abnormal cilia function[1, 14]. All of these cells were subjected to cell sorting to obtain only those with normal chromosomal numbers. However, the rate of polyploidy or aneuploidy remains relatively constant in our mutant cells or human PKD cells. If we were to sort for polyploidy, they would not propagate further in culture. If we were to sort for diploidy, the polyploidy would appear within six passages, or even earlier. Thus, we believe that the “normal” PKD cells

will eventually become polyploidy or aneuploidy in a matter of time. In some cases, fluid-shear stress was applied to the surface of fully differentiated and confluent cells as previously described[13, 14].

Transfection study

For survivin-GFP experiments, human full-length survivin construct was inserted into pEGFPc1 (*Clontech, Inc.*) as previously described[11]. Cells were transiently transfected with the construct with Fugene 6, according to the manufacturer's instructions (*Roche Diagnostics, Inc.*). About 24 hours after transfection, cells expressing GFP were randomly selected for immunolocalization studies. For siRNA knockdown experiments, we purchased pre-designed commercially available siRNAs that have been previously characterized for PKC (*Santa Cruz Biotechnology, Inc.;* cat.#sc-29449), Akt (*Cell Signaling Inc.;* cat.#6211), aurora-A (*Ambion, Inc.*; cat.#s202070) and survivin (*Ambion, Inc.*; cat#s62463). All siRNAs were used at 10 μM and transfected into cells using Lipofectamine RNAiMAX following the manufacturer's protocol (*Invitrogen Inc.*).

Organ cultures

For *in vitro* analysis, we isolated kidneys from wild-type E15.5 mice. Individual kidney was then cultured on the transwell filter. DMEM culture medium containing 4 mM glutamine, 1X penicillin/streptomycin, 5 mg/mL insulin, 5 mg/mL transferrin and 5 ng/mL selenium was used in the absence or presence of 50 μM EM-1451 (*Erimos Pharmaceutics, Inc.*) or 100 μM VE-465 (*Merck, Inc.*). These concentrations were determined to be optimal conditions through dose-response studies (data not shown). The medium was supplied from underneath the transwell or the base of the filter to feed the kidney tissue. The medium was changed every day after

micrography of the kidneys with Nikon TE2000 microscope equipped with a color camera. Unless otherwise indicated, all culture media were obtained from *Fisher, Inc.*

Western analysis

Cultured cells were lysed with radioimmunoprecipitation assay (RIPA) buffer, and mouse kidneys and human kidney tissues were homogenized with RIPA buffer. Intracellular contents were collected by centrifugation at 100 *g* for 10 minutes. Total cell lysates were analyzed with a standard 8% SDS-PAGE. For protein isolation and Western analysis from zebrafish embryos, pooled embryos injected with control*MO, pkd2MO, pkd2MO* plus *survivin* mRNA, *survivin* mRNA alone, or *pkd2MO* plus VEGF were dechorionated and deyolked manually at 28 hpf stage and lysed with RIPA buffer containing protease inhibitor cocktail (*Roche*, Inc.). After determination of protein concentration (BCA assay kit, *Fisher Scientific*, Inc.), 50 μg of protein extract was loaded onto a 12% SDS-PAGE gels and transferred to nitrocellulose membranes.

The following primary antibodies were used for Western. pNF-κB (1:250), Akt (1:1,000), p-Akt (1:250), GAPDH (1:1,500), and cyclin-B1 (1:1,000) were obtained from *Cell Signaling, Inc.*; NF-κB (1:500) from *Santa Cruz Biotechnology Inc.*; aurora-A (1:1,000) from *BD Transduction, Inc.*; survivin (1:500) from *Novus Biologicals, LLC*; and actin (1:1,000) from *Sigma, Inc.*

Immunostaining study

Both actively dividing and fully differentiated cells were stained with various antibodies to study protein translocations and subcellular localizations. Longitudinal sections from mouse kidneys and aortas were also studied for cell division and mitotic spindle orientation. Briefly, cells and

tissues were fixed with 4% paraformaldehyde in 2% sucrose solution for 10 minutes at room temperature. After primary and secondary antibodies had been applied, samples were sandwiched on the microscope slide. They were observed with an inverted Nikon Ti-U microscope and analyzed three dimensionally with Metamorph 7.0. We have recently published a more detailed protocol and analysis of the longitudinal sections[15]. In some cases, a standard H&E and lectin staining was carried out. For zebrafish, whole-mount immunocytochemistry was performed using JB4 resin according to the manufacturer's instructions (Polyscience, Inc., Warrington, Philadelphia). Four-micron sections were cut by a Leica RM2255 microtome (Leica, Buffalo Grove, Illinois). Phenotypes were scored with a Nikon SMZ800 stereomicroscope equipped with a QImaging MicroPublisher 5.0 RTV color CCD camera operated by QCapture software.

Some kidney sections were immunostained with ZO-1, DBA (*dolichos biflorus* agglutinin) and WGA (wheat-germ agglutinin). ZO-1 recognizes tight junctions of renal epithelia; DBA is a lectin used as a marker for renal collecting ducts; WGA is a lectin found in all convoluted tubules as well as glomeruli in the kidney. We used these markers to generate contrast and indicate individual tubules in the renal phenotypic analyses. While ZO-1 was used in our planar cell polarity to highlight directions of tubular axes, DBA and WGA were used to indicate cyst or lumen areas. For the planar cell polarity analysis, we only counted dividing cells and measured the angle of nuclear division orientation relative to the orientation of the tubular axis as revealed by ZO-1 staining. For lumen/cyst areas, we measured lumen areas in DBA and/or WGA-positive cysts in both wild-type and *Mx1Cre:Survivin*$^{flox/flox}$ control and surgical kidney sections. Image acquisition and analysis were done with Metamorph 7.0.

Anti-survivin (1:500), aurora-A (1:1,000), NF-κB (1:500) antibodies were used for immunostaining. Antibodies purchased from *Vector Laboratories, Inc.* include rhodamine-labeled DBA (1:100), fluorescein-labeled WGA (1:100), rhodamine-conjugated phalloidin (1:500), and DAPI (1X). Other antibodies include pericentrin (1:1,000; *Covance, Inc.*), acetylated-α-tubulin (1:1,000; *Sigma, Inc.*), and ZO-1 (1:100; *ABCam, Inc*.).

Flow cytometry analysis

Cultured cells or freshly isolated cells from human, mouse and zebrafish were used in flow cytometry experiments. In some cases, cells were incubated with 30 μM 5-bromo-deoxyuridine (BrdU; *Sigma, Inc.*) for 15 minutes and rinsed with 1X PBS. The DNA was then denatured at 97 °C for 15 minutes and quickly chilled in an ice-water bath for 15 minutes. Anti-BrdU Alexa Fluor488 antibody was used at dilution of 1:100 (*Invitrogen, Corp.*). In apoptotic experiments, FITC conjugated annexin V antibody was used at dilution 1:100 (*Invitrogen, Inc*.). Propidium iodide at concentration of 20 μg/ml (PI; *Sigma, Inc.*) with or without counter-staining of phospho-Histone3B antibody (*Sigma, Inc.*) at dilution 1:100 was used in other experiments. Cells were analyzed with C6 Flow Cytometer (*Accuri Cytometers, Inc.*) using FL1, FL2 or FL3 detector to measure different fluorophore intensities.

Chromosomal analysis

Individual cells were isolated and incubated with 0.05 mg/ml colcemid solution for 30 minutes at 37 °C. The cells were incubated with 0.56% KCl solution for 45 minutes at 37 °C, followed by fixing with 3:1 (v/v) methanol:acetic acid. Individual cells were dropped onto a pre-cleaned

glass slide and counter stained with DAPI. After sequential digestion with RNase and pepsin, the chromosomal DNA on the slide was denatured in 70% formamide and then hybridized with a cocktail of mouse or human SKY paint probes tagged with various nucleotide analogues according to the procedure recommended by *Applied Spectral Imaging*, Inc. (ASI; Vista, CA). The images from combinations of five different fluorophores were developed and analyzed. Rhodamine, Texas-Red, Cy5, FITC and Cy5.5 were captured with a spectral cube and interferometer module installed on an Olympus microscope. Spectral-Karyotypes were carried out using SKY View software (Version 1.62).

For zebrafish chromosome spreading, eggs were collected at the two-cell stage and injected with control*MO*, *pkd2MO*, *pkd2MO* plus *survivin* mRNA, *survivin* mRNA alone, or *pkd2MO* plus VEGF. Because these cells were actively dividing and developing into embryos at this period, three hours incubation was sufficient for the morpholinos, mRNA or VEGF to take effect. These three-hours postfertilization (hpf) eggs contained about 1,000 cells. Next, 0.02% colchicine was added for an additional four hours before the choriones were removed with protease solution. De-chorionated embryos were then incubated in 0.56% KCl solution for 40 minutes and fixed with 3:1 (v/v) methanol:acetic acid solution for 20 minutes. Chromosomes were spread on the slide for analysis after DAPI staining. Because zebrafish chromosome-specific probes for chromosomal spectral karyotype analysis are not available, we characterized individual chromosomes based on the ideogram derived from the replication banding of *Danio rerio*[16].

Live-imaging study

Primary renal epithelial cells or vascular endothelial cells were transfected with or without *Survivin* siRNA. Cells were then incubated with membrane-permeable and DNA-specific dye, Hoechst for 20 minutes. One Randomly selected cells from each group were studied and recorded with a Nikon TE2000 microscope equipped with an environmental chamber. Hoechst fluorescence and high-resolution differential interference contrast images were captured every 2-5 minutes at exposure time of 500 and 100 milliseconds, respectively. For better focusing, the microscope was equipped with XY-axis motorized flat top inverted stage, automatic focusing RFA Z-axis drive, and custom-designed vibration isolation platform. For a better-controlled environment, the body of the microscope was enclosed inside a custom-built chamber to control CO_2, humidity, heat and light.

Zebrafish study

Wild-type (wt) zebrafish AB strains were maintained according to standard protocols used to maintain and raise wt strains and embryos. Embryos were cultured at 28.5°C in 0.0045% phenylthiourea in a Danieau buffer to inhibit pigmentation. Zebrafish embryos were microinjected at the 1-2 cell stage with 1 mM antisense morpholino (*MO*) oligonucleotides obtained from GeneTools (Philomath, OR). A volume of 1 nL of *pkd2MO* (translational blocking *MO*) that targets against the 5'UTR of *pkd2* (*pkd2MO:* 5′-AGG ACG AAC GCG ACT GGA GCT CAT C-3′) was injected using a Narishige IM-9B microinjector (East Meadow, New York) controlled by a Narishige NAI-2N micromanipulator (East Meadow, New York) to deliver 9.0 ng into the embryo. As a control, zebrafish embryos were injected with 1-2 nL of *controlMO* (5′-CCT CTT ACC TCA GTT ACA ATT TAT A-3′) to deliver 6-12 ng into the embryo. Note

that both of these *MO*s have been previously utilized[17-19]. Un-injected control embryos were also used to verify the studies (data not shown). For rescue experiments, full-length human survivin gene (without GFP) was cloned in the survivin vector as described previously[11]. After linearization, the plasmids were transcribed *in vitro* with T7 RNA polymerase using the mMESSAGE mMACHINE kit from *Ambion* (Austin, TX, USA). 100 pg of purified *survivin* mRNA were either co-injected with *pkd2* morpholinos or alone into the 1-2 cell-stage embryos. In another case, 2.5 ng vascular endothelial growth factor (VEGF) was co-injected with *pkd2* morpholinos.

SUPPLEMENTAL FIGURE & FIGURE LEGENDS

Supplemental Figure 1a

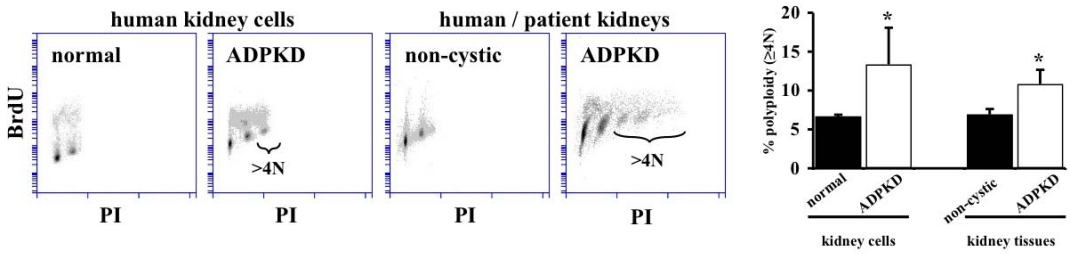

Supplemental Figure 1b

normal kidney cell (46, XY)

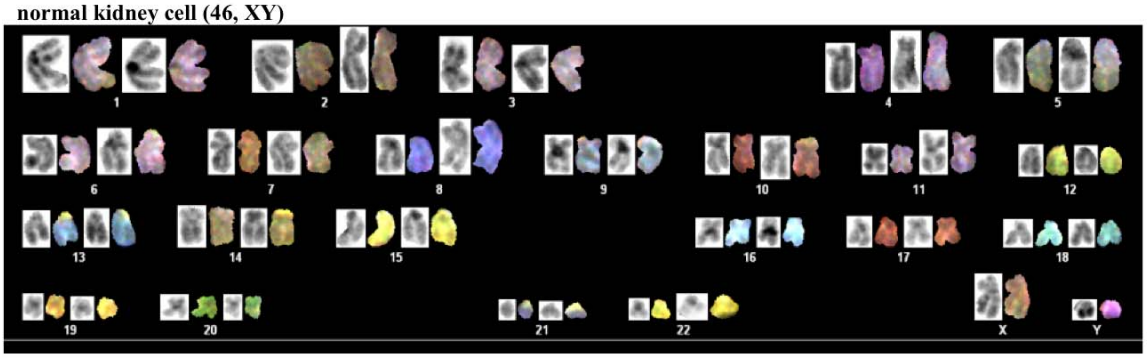

ADPKD kidney cell (45, XY, -4)

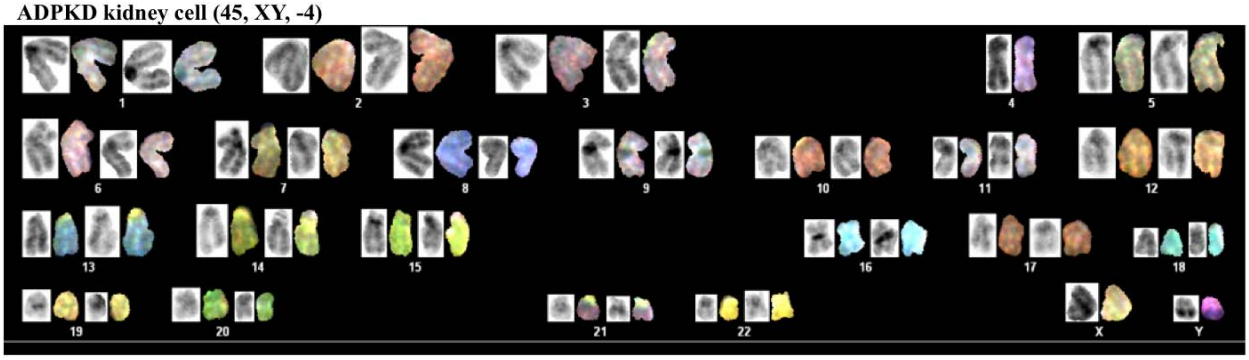

kidney cell line	normal	tetraploidy	aneuploidy	count (N)	% abnormal
non-ADPKD	9	0	2	11	18
ADPKD	20	1	6	27	26

Supplemental Figure 1c

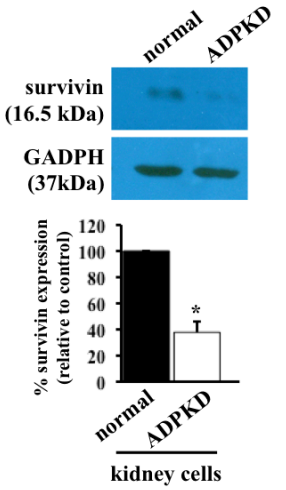

Supplemental Figure 1d

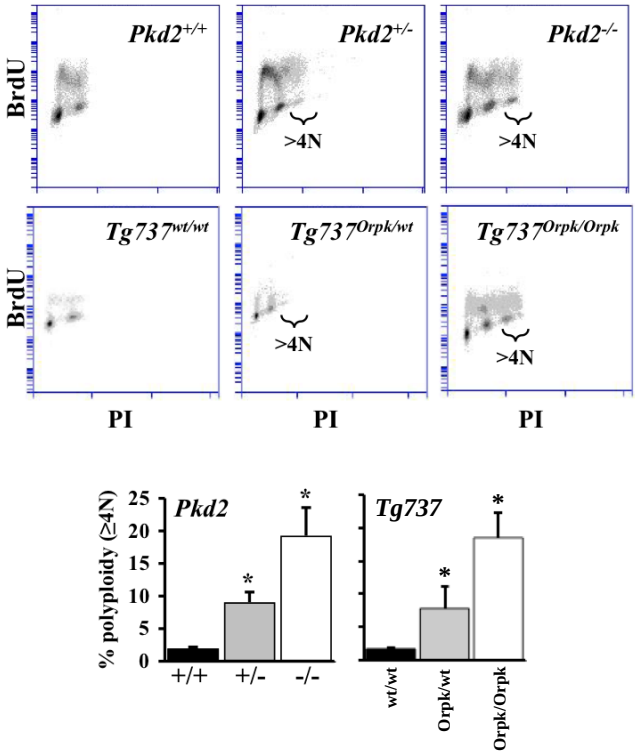

Supplemental Figure 1e

Pkd2$^{+/+}$ (40, XX)

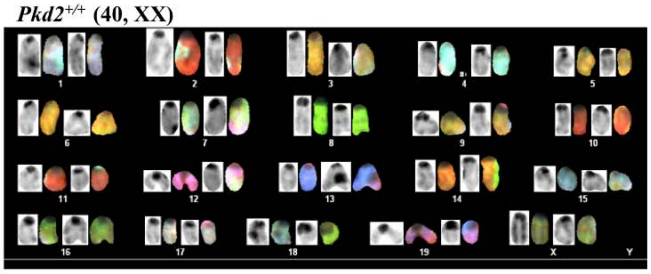

Pkd2$^{-/-}$ (80, XXYY)

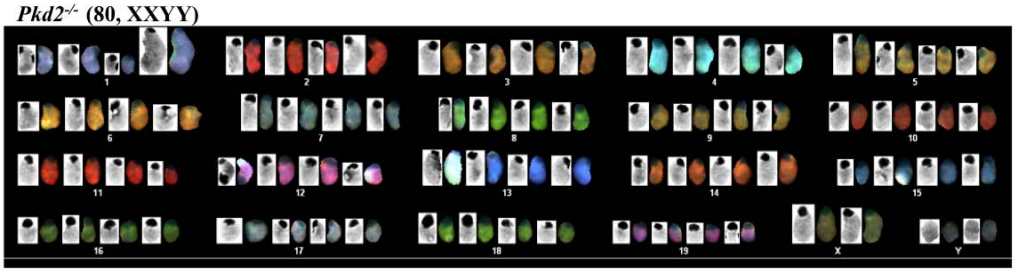

Pkd2$^{+/-}$ (160, XXXXXXXX)

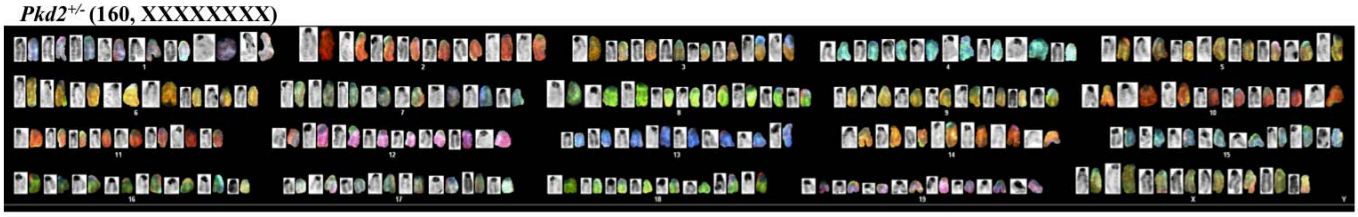

samples		normal	tetraploidy	aneuploidy	count (N)	% abnormal
mouse kidneys	*Pkd2*$^{+/+}$	19	2	0	21	9
	Pkd2$^{+/-}$	8	12	1	21	62
	Pkd2$^{-/-}$	11	13	1	25	56

Supplemental Figure 1f

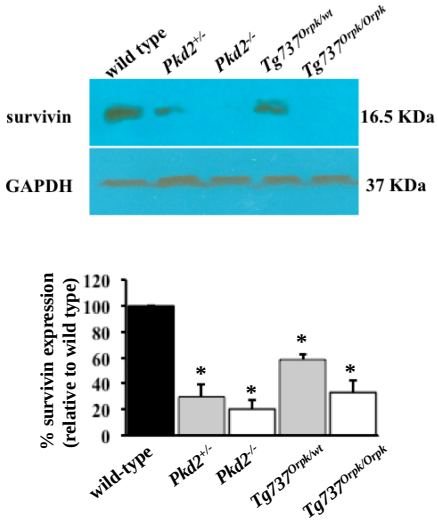

Supplemental Figure 1. Human ADPKD and mouse *Pkd* kidney epithelia are characterized by abnormal ploidy level and survivin down-regulation.

(**a**) Previously characterized human cell lines from normal and ADPKD kidneys were analyzed for their cellular divisions with flow cytometry by BrdU and PI staining. We first pre-sorted and collected only diploid cells (2N). Over the next 5-10 passages, we observed that compared to non-cystic cells, ADPKD-derived cells have a greater chance of producing genetic instability in their chromosomal composition. Bar graph shows that epithelia from both *ADPKD* kidney cells contain a greater polyploidy with DNA content of >4N compared to non-ADPKD or normal ones. (**b**) Further karyotype analysis of individual cells confirms the presence of abnormal genomic compositions (aneuploidy or polyploidy) in ADPKD cells. (**c**) Human cell lines were also used to confirm survivin expression, and GADPH was used as loading control. Bar graph shows relative survivin expression levels. (**d**) Representative BrdU and PI labeling profiles reveal an increase in cell polyploidy in kidneys from both heterozygous (*Pkd2*$^{+/-}$ or *Tg737*$^{Orpk/wt}$) and homozygous (*Pkd2*$^{-/-}$ or *Tg737*$^{Orpk/Orpk}$) mice compared to the corresponding wild-type (*Pkd2*$^{+/+}$ or *Tg737*$^{wt/wt}$). Bar graph shows that epithelia from both *Pkd2* and *Tg737* kidneys, compared to their wild-type kidneys, significantly contain greater polyploidy with DNA content of >4N. (**e**) Karyotyping was carried out in freshly isolated cells from *Pkd2*$^{+/+}$, *Pkd2*$^{+/-}$ and *Pkd2*$^{-/-}$ kidneys to visualize individual chromosomes. A simple chromosome count indicates the presence of polyploidy cells in both *Pkd2*$^{+/-}$ and *Pkd2*$^{-/-}$ kidneys. Further characterization of individual chromosomes with fluorescence probes indicates the polyploid and aneuploid nature of *Pkd2*$^{+/-}$ and *Pkd2*$^{-/-}$ kidneys. (**f**) Embryonic kidneys were pooled and analyzed for survivin expression, and GAPDH was used as loading control. Bar graph shows relative survivin

expression levels. For flow cytometry and Western experiments, N≥4 for independent kidney isolations for each genotype (analyzed with ANOVA test followed by Dunn's Multiple Comparison posttest analysis) and each human cell line (analyzed with paired Student *t*-test).

Supplemental Figure 2a

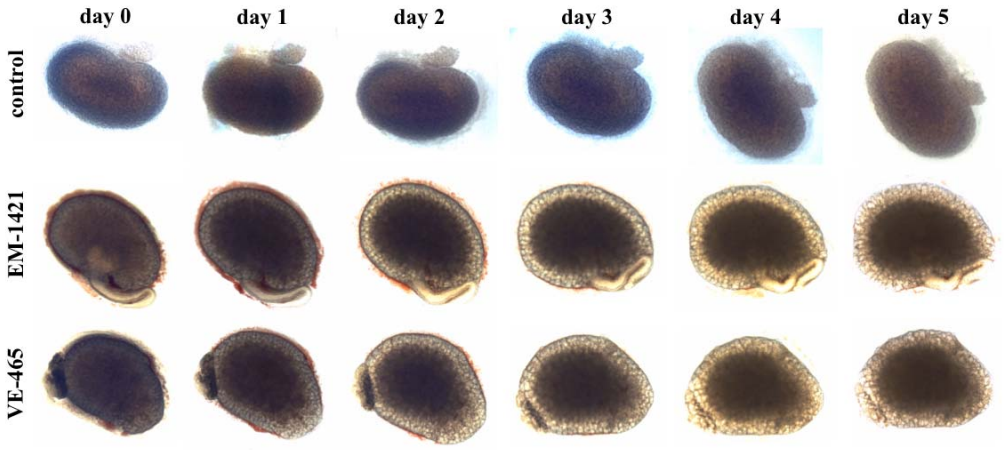

Supplemental Figure 2b

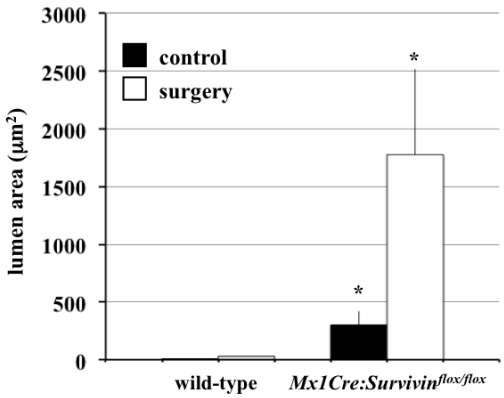

Supplemental Figure 2c

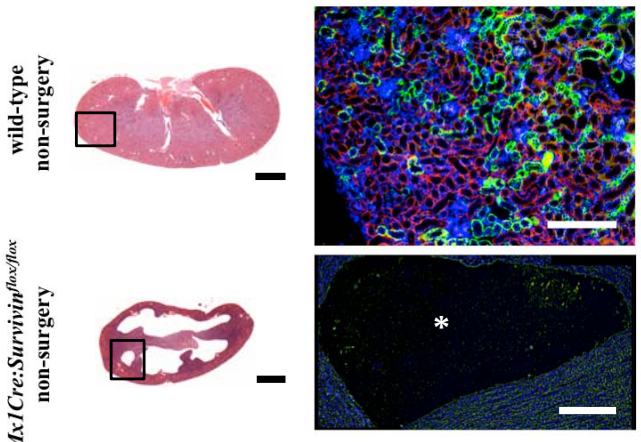

Supplemental Figure 2. Survivin downregulation is sufficient to induce cystic kidney formation.

(**a**) Embryonic kidneys from E15.5 of the same litter were isolated and cultured on transwell filters. After the first micrographs were taken at day 0, cultures were then treated with vehicle as control, 50 μM EM-1451 or 100 μM VE-465 to induce abnormal cell division by inhibiting survivin or aurora-A kinase, respectively. Kidney cultures were micrographed daily for a total of six days. Cyst-like phenotype was apparent as early as day 2. (**b**) Bar graph shows quantitation of lumen sizes (cyst areas) in wild-type and *Survivin* knockout kidneys. A total of 30-53 lumen areas were measured from three randomly selected kidneys in each group. (**c**) Paralleled kidney sections were obtained from three-months old mice for H&E and fluorescence analyses. Box in the H&E kidney corresponds to an approximate area for further fluorescence study. White asterisk indicates renal cyst. N≥3 for kidney analysis in each group and genotype (analyzed with ANOVA test followed by Dunn's Multiple Comparison posttest analysis). White bar=200 μm; black bar=1 mm.

Supplemental Figure 3a

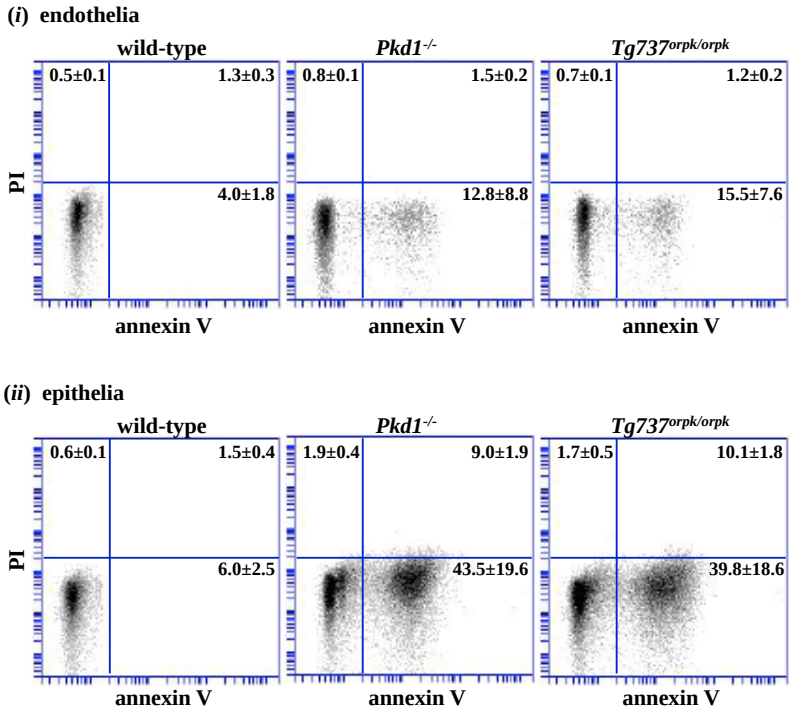

Supplemental Figure 3b

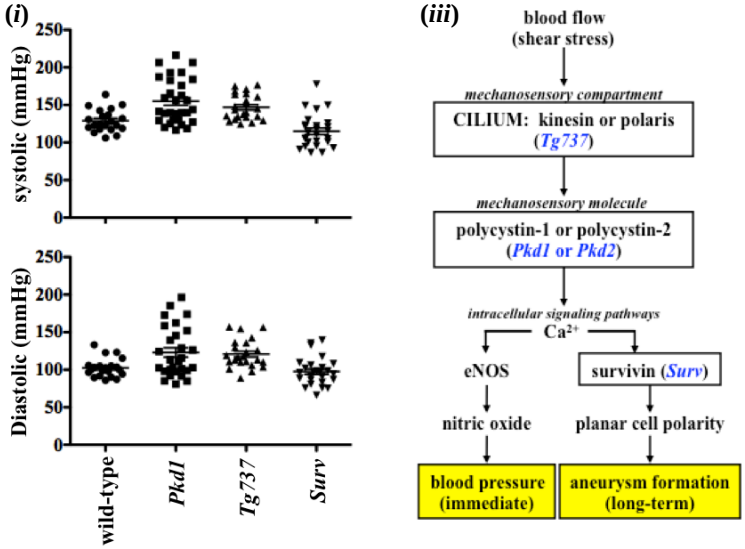

(*ii*)

	systolic (mmHg)	diastolic (mmHg)	N
wild-type	128±9	102±7	3
Pdgfbcre:Pkd1$^{flox/flox}$	150±19*	120±21*	4
Tie2Cre:Tg737$^{flox/flox}$	147±10*	120±11*	3
Pdgfβcre:Surv$^{flox/flox}$	114±13	99±13	3
** significant different from wild-type control*			

Supplemental Figure 3. Apoptosis and blood pressure measurements.

(**a**) Compared to the corresponding control wild-type cells, apoptosis is significantly greater in vascular endothelial (***i***) and renal epithelial (***ii***) of *Pkd1* and *Tg737* mutant cells. Annexin V is used as an early apoptotic marker, and propidium iodide (PI) is used as a necrotic marker. (**b**) *Pdgfβcre:Survivin*$^{flox/flox}$ mice do not have elevated systolic or diastolic blood pressure. Blood pressure was measured in wild-type and conditional *Pkd1*, *Tg737*, and *Survivin* (*Sur*) mice for a 2-week period (***i***). The averaged measurements of blood pressure during this 2-week period were tabulated (***ii***). A working model is presented showing the roles of primary cilia in blood pressure and aneurysm formation (***iii***).

Supplemental Figure 4a

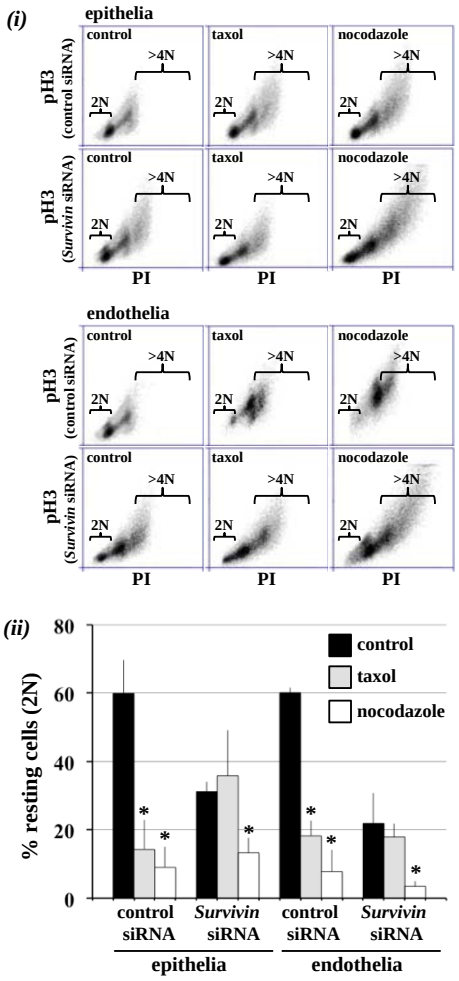

Supplemental Figure 4b

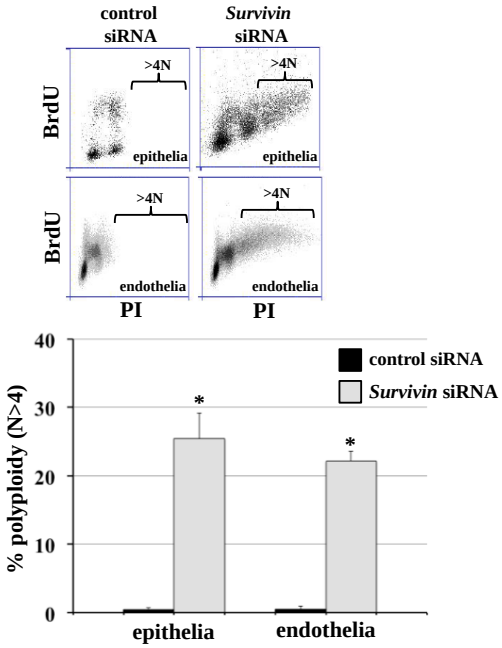

Supplemental Figure 4. Survivin down-regulation is associated with abnormal cytokinesis in primary cells of renal epithelia and vascular endothelial cells.

(**a-*i***) Mitotic-stress test indicates abnormal cytokinesis associated with knockdown of a chromosomal passenger protein (survivin). Cell-cycle arrest was induced with taxol or nocodazole to stabilize or depolymerize mitotic spindles, respectively. Those cells with abnormal chromosomal passenger protein expression were not inhibited in cell arrest-induced by taxol. Phospho-histone3b (pH3) and PI were used to differentiate those cells that were not arrested by taxol. (**a-*ii***) Mitotic stress was measured by analyzing changes in resting cells (2N), which are PI- and pH3-negative, from the total cell population. The test would thus examine if survivin down-regulation is responsible for a cell escaping cell-cycle arrest in the presence of taxol. The results from the mitotic-stress test indeed indicate that knockdown of survivin expression was characterized by abnormal cytokinesis. Although most normal cells could be arrested by nocodazole (microtubule depolymerizer) and taxol (microtubule stabilizer), survivin knockdown cells could only be arrested by nocodazole. This is consistent with previous reports showing that cells with abnormal chromosomal passenger complex, such as survivin, would not be arrested by taxol. (**b**) To validate that *Survivin* knockdown would induce abnormal cytokinesis leading to polyploidy, cell-cycle profile was analyzed with PI and BrdU to study cellular proliferation in epithelial and endothelial cells. Bar graph shows that compared to corresponding control groups, survivin knockdown-epithelia and endothelia contain significantly more polyploidy with DNA content of >4N. Bar=50 μm. $N \geq 3$ for each group and treatment (analyzed with ANOVA test followed by Dunn's Multiple Comparison posttest analysis).

Supplemental Figure 5a

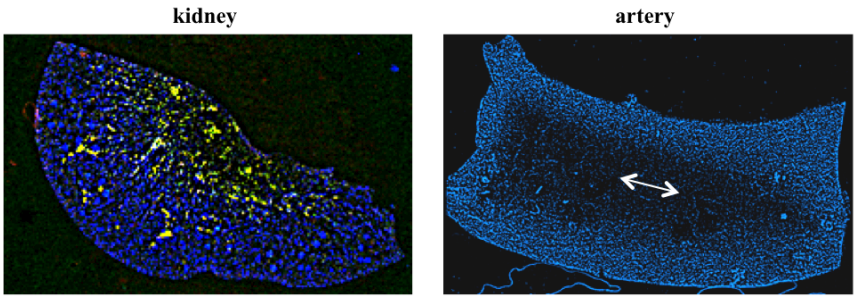

Supplemental Figure 5b

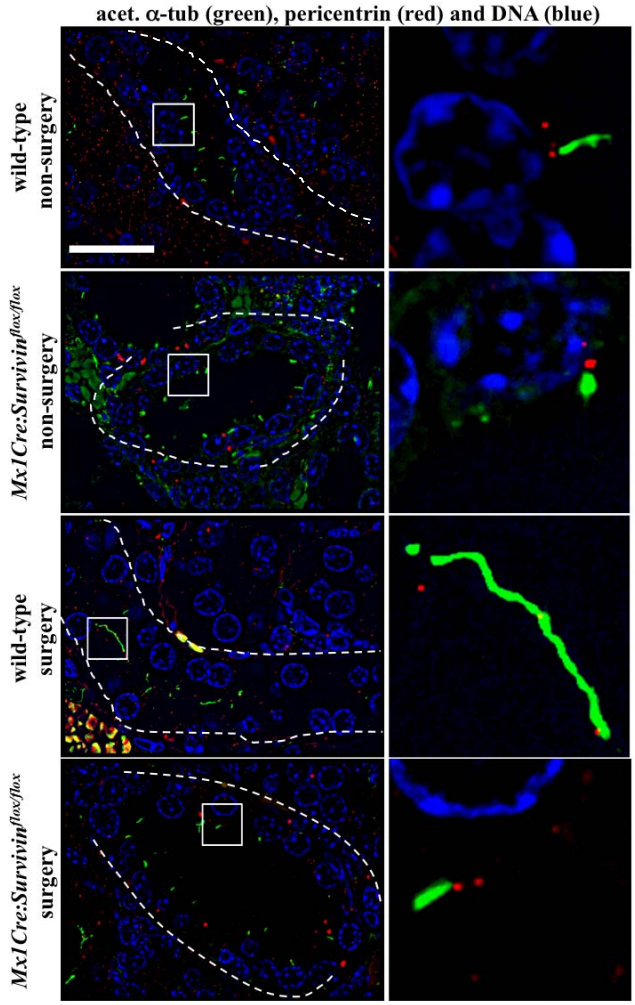

Supplemental Figure 5c

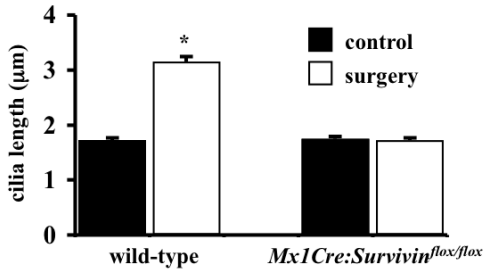

Supplemental Figure 5d

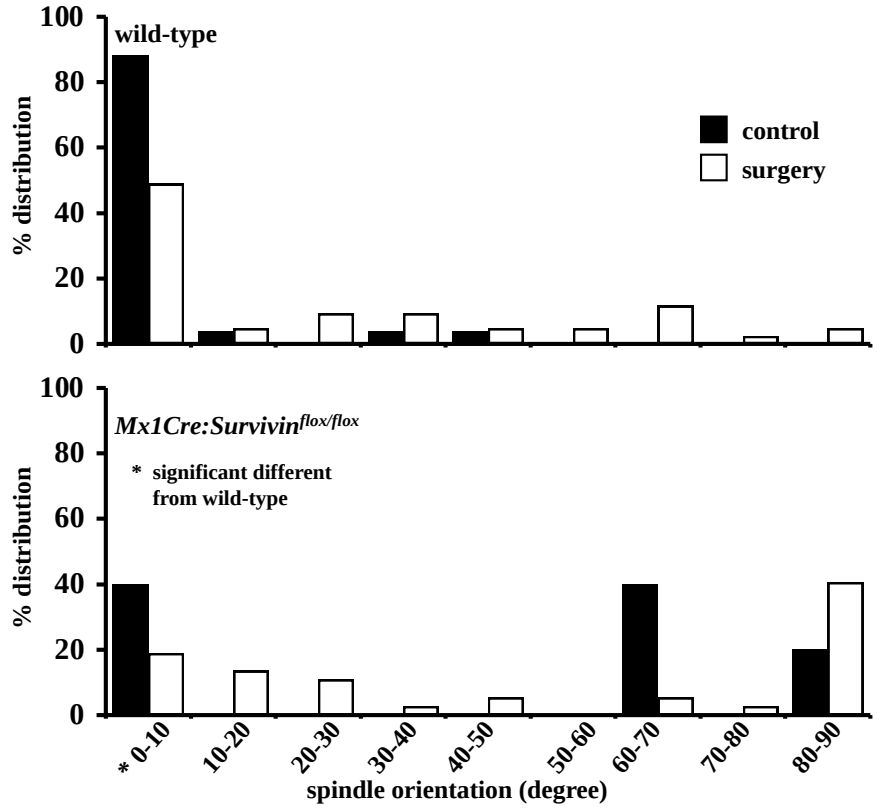

Supplemental Figure 5. Abnormal cellular division orientation is associated with renal cystic and vascular aneurysm phenotypes.

(**a**) Mouse kidney and artery longitudinal sections stained with acetylated-α-tubulin (green), pericentrin (red), and DAPI (blue) were used to examine cell division orientation. (**b**) Longitudinal kidney tubular sections from wild-type and *Mx1Cre:survivin*$^{flox/flox}$ mice with or without UUO surgery were used to study structural length of primary cilia. Longer cilia were observed in tubular sections of wild-type UUO kidneys. White box indicates the enlargement of the region within the kidney lumen. (**c**) The length of cilia in wild-type kidney tubules was significantly increased following UUO surgery but not in *Mx1Cre:survivin*$^{flox/flox}$ mice. (**d**) The frequency distribution of cell-division orientation angle (degrees) was tabulated in control and surgical kidneys in both wild-type and *Mx1Cre:survivin*$^{flox/flox}$ mice. Angles of cell-division orientation in *Mx1Cre:survivin*$^{flox/flox}$ mice show a shift towards the higher angle groups in both control and surgical kidneys. N≥3 for each group and genotype. N≥100 for distribution of spindle orientation angle for each genotype and each treatment. N≥1,600 for cilia length measurement. Bar=40 μm.

Supplemental Figure 6a

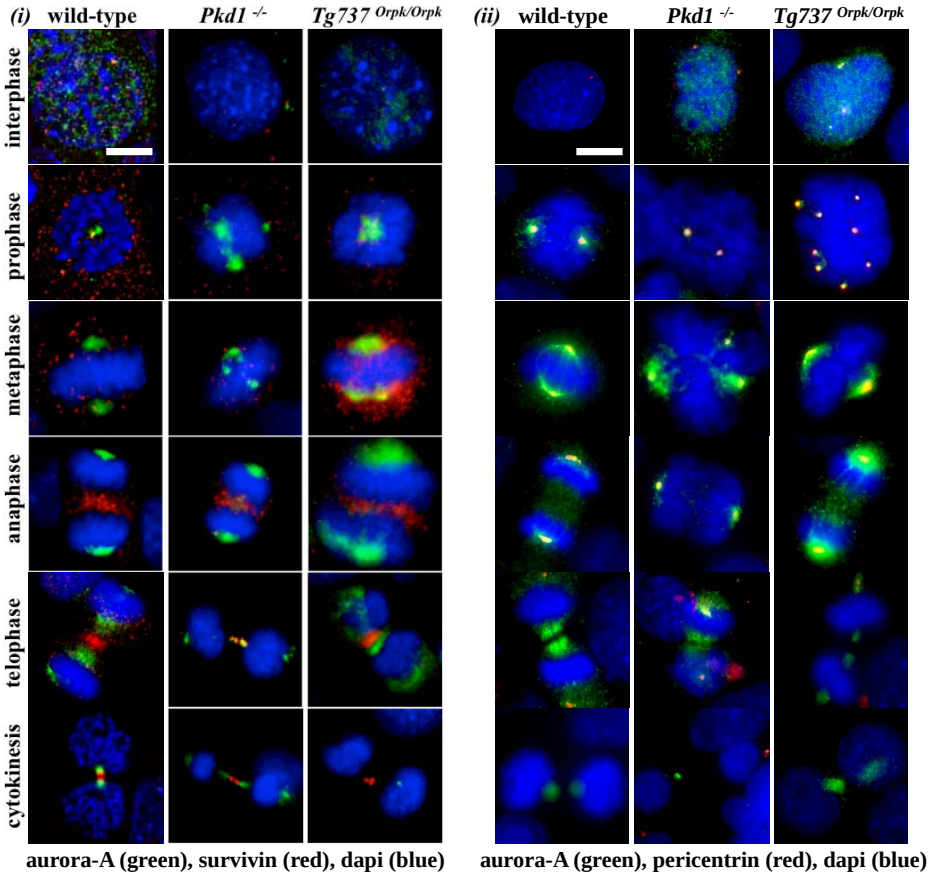

Supplemental Figure 6b

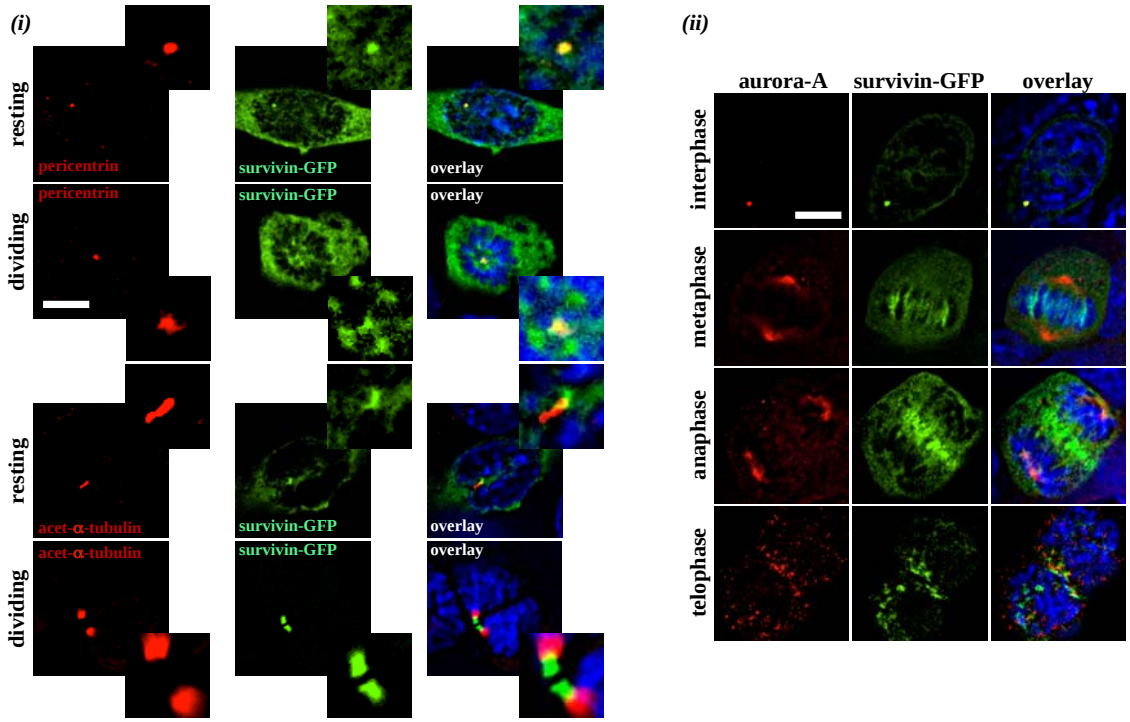

Supplemental Figure 6. Confirmations of survivin antibody and survivin/aurora-A localization. (**a**) Cells were stained with aurora-A (green) and survivin (***i***; red) or pericentrin (***ii***; red). To study subcellular localization of aurora-A and survivin, images were captured at different cell-cycle stages of interphase, prophase, metaphase, anaphase, telophase and cytokinesis. Aurora-A and survivin are localized to the centriole in interphase, the centrosome in prophase and the mid-body during telophase and cytokinesis. (**b**) Cells were transfected with survivin-GFP (green) and stained with pericentrin/acetylated-α-tubulin (***i***; red) or aurora-A (***ii***; red). Subcellular localizations of survivin/aurora-A were studied in resting and dividing cells. Insert shows area of enlargement for survivin/pericentrin/acetylated-α-tubulin localization. Bar=10 μm.

Supplemental Figure 7a

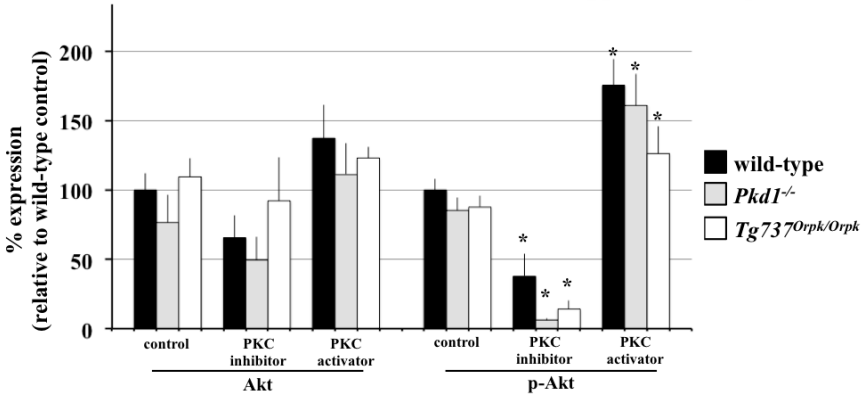

Supplemental Figure 7b

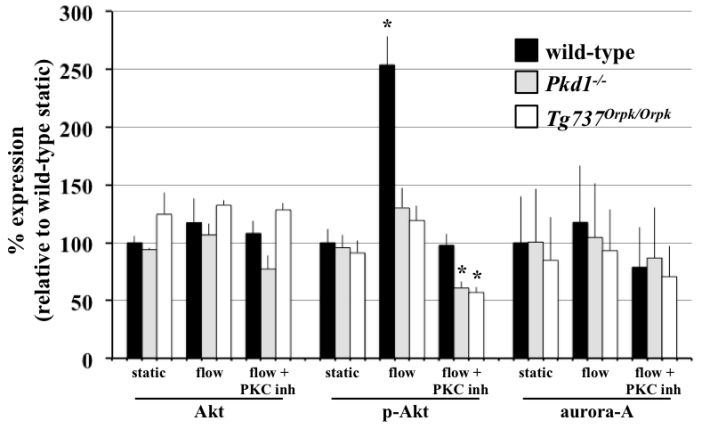

Supplemental Figure 7c

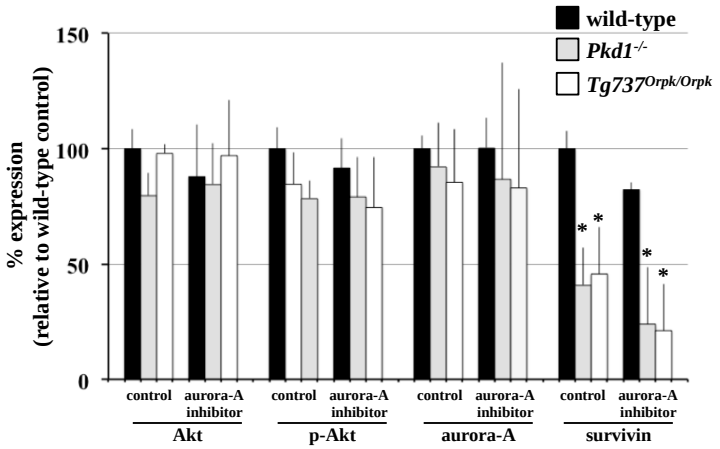

Supplemental Figure 7d

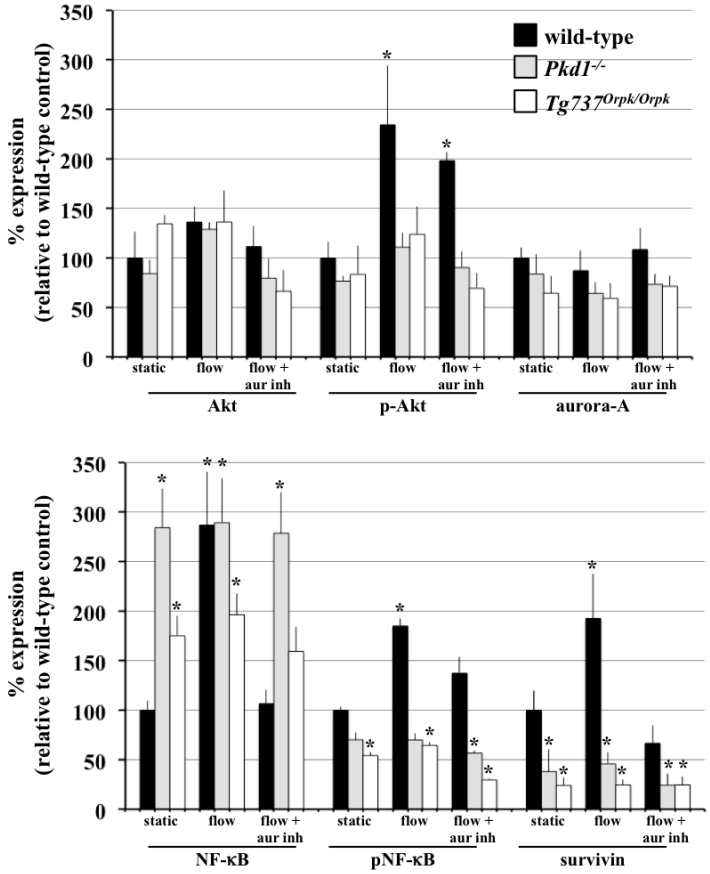

Supplemental Figure 7e

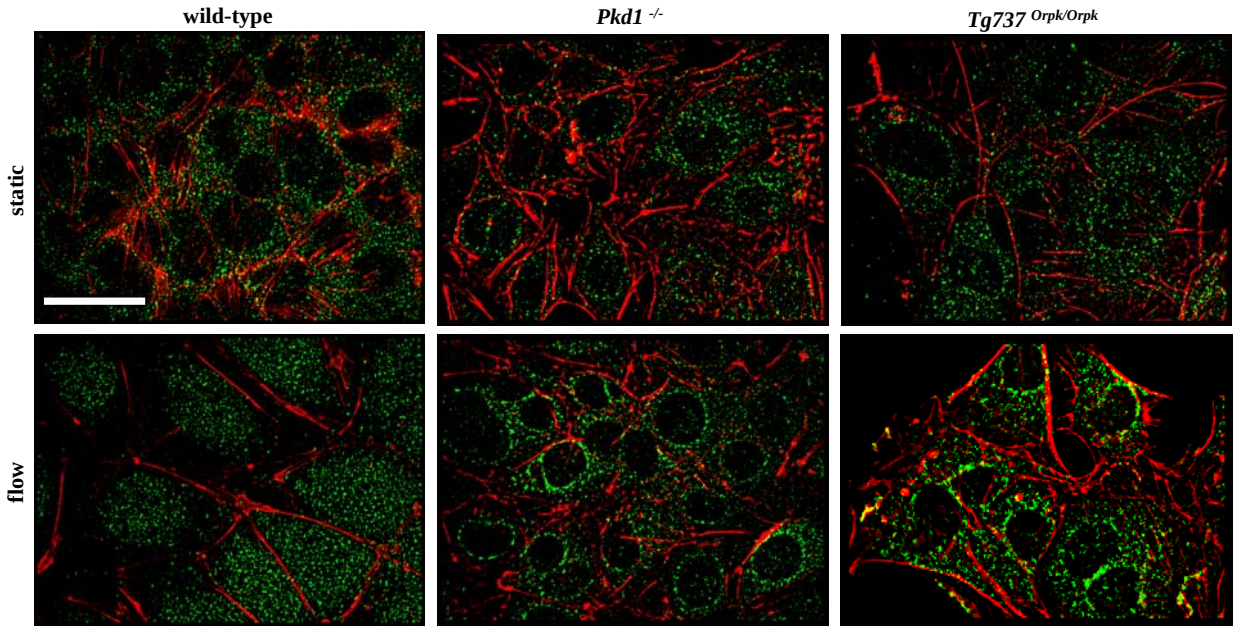

NF-κb (green), actin (red)

Supplemental Figure 7f

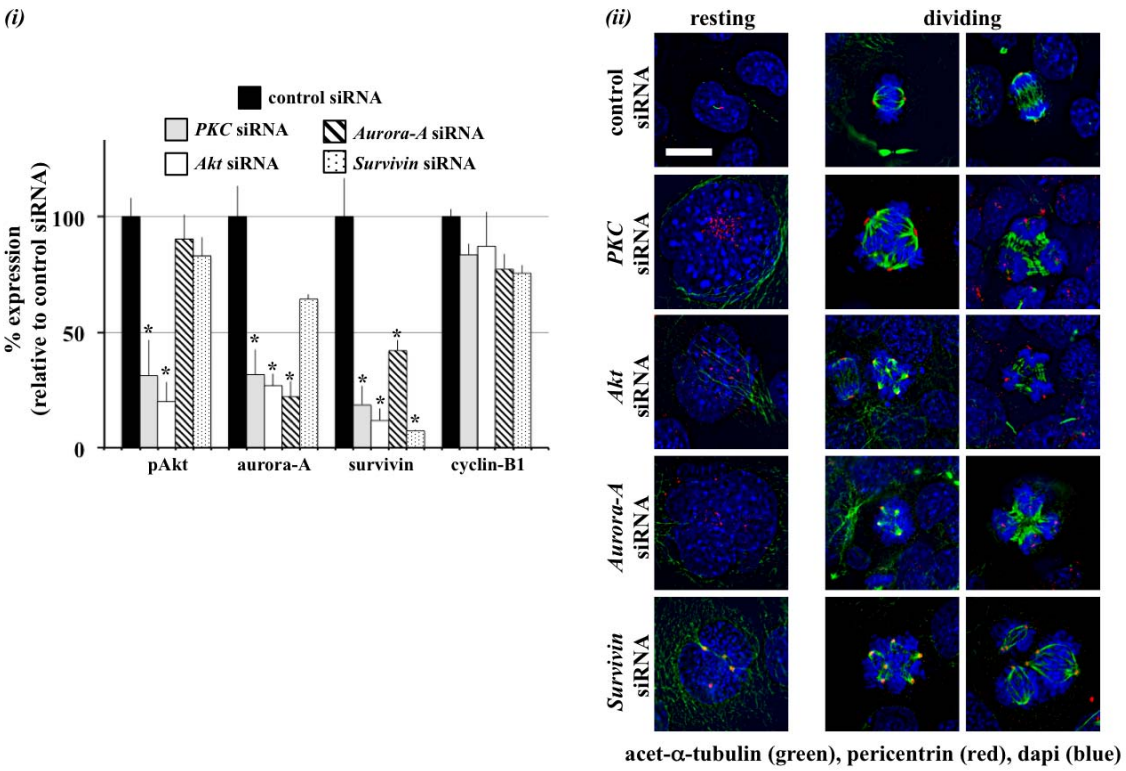

Supplemental Figure 7g

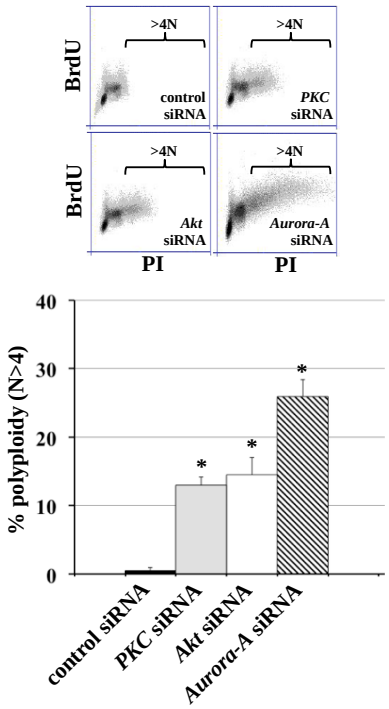

Supplemental Figure 7. PKC/Akt/NF-κB signaling pathway regulates flow-induced survivin expression and cell division.

(**a**) After wild-type and cilia mutant (*Pkd1*$^{-/-}$ and *Tg737*$^{Orpk/Orpk}$) cells were treated with PKC inhibitor or activator, both Akt and p-Akt were analyzed. When treated with PKC inhibitor, all cell lines showed down-regulation of p-Akt, while PKC activator treatment showed an increase in p-Akt compared to non-treated control cells. (**b**) The effect of fluid-flow on Akt and aurora-A expression was analyzed in the presence or absence of PKC inhibitor. When subjected to fluid-shear, p-Akt expression was up-regulated only in wild-type cells. While p-Akt expression returned to basal levels following treatment with PKC inhibitor and fluid-shear stress in wild-type cells, it stayed repressed in mutant cells. (**c**) Treatment with aurora-A inhibitor resulted in a decrease in p-Akt, aurora-A and survivin expression; however, these decreases were not significant from the control, non-treated group. (**d**) While total Akt level was not changed, fluid-shear stress significantly induced expression of p-Akt in wild-type but not in mutant cells. Aurora-A expression was increased following fluid-shear stress in wild-type cells; however, this increase was not significant from control. Both NF-κB and pNF-κB expressions were increased following fluid-shear stress only in wild-type cells, while mutant cells maintained a high basal level of NF-κB compared to static wild-type cells. Survivin expression was increased following shear-stress in wild-type cells. (**e**) NF-κB nuclear translocation was confirmed with immunostaining study. Cells were stained with NF-κB p65 (green), actin (red) to examine subcellular localization of NF-κB before and after fluid flow. In contrast to mutant cells, wild-type cells show NF-κB translocation from cytoplasm to nucleus when subjected to fluid-shear stress. (**f-*i***) Western blot analyses were conducted to confirm the signaling mechanism involving survivin expression by siRNA-mediated knockdown of PKC, Akt, aurora A, or survivin. (**f-*ii***)

To further confirm the involvement of these signaling molecules in centrosome number and cell division abnormality, immunofluorescence analysis was performed using acetylated-α-tubulin and pericentrin. (**g**) Flow cytometry was done to analyze ploidy level in PKC, Akt or aurora-A knockdown cells. Bar=40 μm. N≥3 for each group and treatment. All Western blot analyses were done by comparing treatment groups to their corresponding wild-type control, non-treated groups. Data analysis was performed with ANOVA test followed by Dunn's Multiple Comparison posttest analysis

Supplemental Figure 8a

overall phenotypic observations

28 hpf n/total (%)	curly tail	renal cyst
control *MO*	0/61 (0)	N/A
pkd2 MO	55/70 (79)	N/A
pkd2 + *survivin* mRNA	36/95 (38)	N/A
survivin mRNA	0/53 (0)	N/A
pkd2 + VEGF	22/67 (33)	N/A
48 hpf n/total (%)	**curly tail**	**renal cyst**
control *MO*	0/45 (0)	0/25 (0)
pkd2 MO	36/46 (78)	24/29 (83)
pkd2 + *survivin* mRNA	24/63 (38)	10/26 (38)
survivin mRNA	0/42 (0)	0/25 (0)
pkd2 + VEGF	30/67 (45)	14/28 (50)
72 hpf n/total (%)	**curly tail**	**renal cyst**
control *MO*	0/45 (0)	0/27 (0)
pkd2 MO	36/46 (78)	23/26 (88)
pkd2 + *survivin* mRNA	28/61 (46)	19/28 (68)
survivin mRNA	0/42 (0)	0/21 (0)
pkd2 + VEGF	45/67 (67)	19/26 (73)

Supplemental Figure 8b

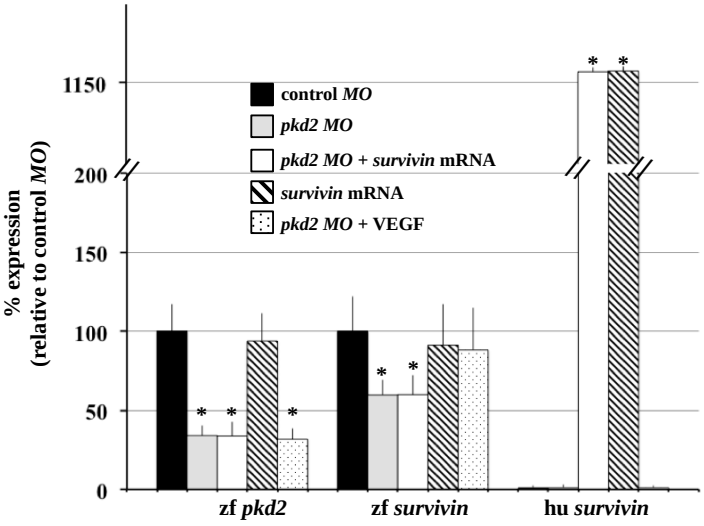

Supplemental Figure 8c

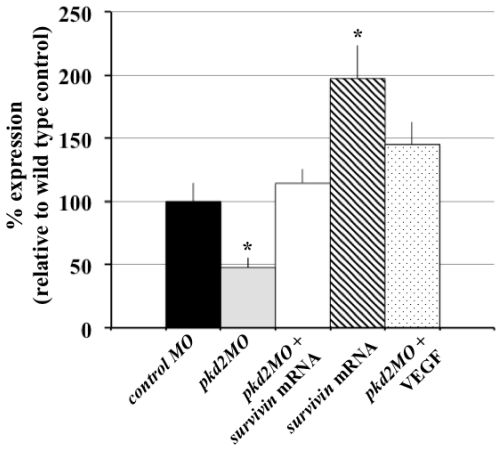

Supplemental Figure 8d

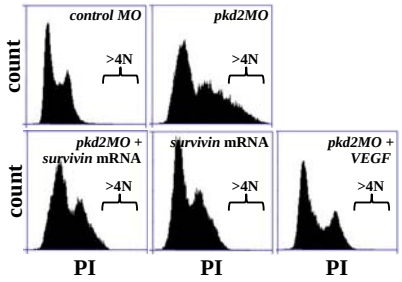

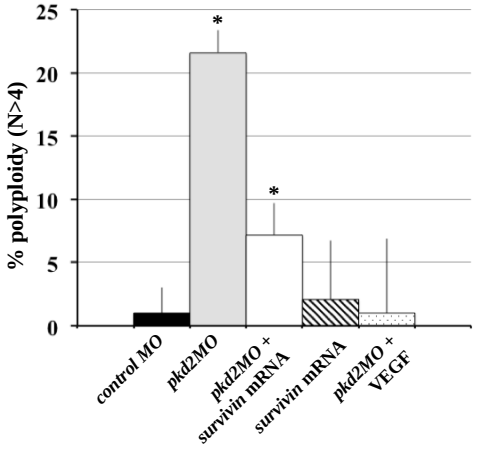

Supplemental Figure 8. Survivin overexpression rescued PKD phenotypes in zebrafish.

(**a**) An overall phenotypic was tabulated for wild-type, curly tail and renal cyst phenotypes in zebrafish injected with either control *MO*, *pkd2* MO, *pkd2 MO* plus *survivin* mRNA, *survivin* mRNA alone, or *pkd2 MO* plus VEGF. (**b**) RT-PCR was performed to examine zebrafish (zf) and human (hu) transcript levels for *survivin* and to confirm *pkd2* knockdown. Human survivin was introduced through mRNA injection. α-tubulin was used as a loading control. (**c**) Expression levels of survivin were analyzed in all the groups, in which zebrafish and human survivin can be recognized by the same antibody. (**d**) Polyploidy level was also validated and quantified with flow cytometry by isolating cells from each group of zebrafish. $N \geq 4$ for each group and treatment. All Western blot and RT-PCR analyses were done by comparing injected groups to the control *MO* group. Data analysis was performed with ANOVA test followed by Dunn's Multiple Comparison posttest analysis

SUPPLEMENTAL REFERENCES

1. Xu C, Shmukler BE, Nishimura K, Kaczmarek E, Rossetti S, Harris PC, Wandinger-Ness A, Bacallao RL, Alper SL. Attenuated, flow-induced atp release contributes to absence of flow-sensitive, purinergic cai2+ signaling in human adpkd cyst epithelial cells. *American journal of physiology*. 2009;296:F1464-1476
2. Wu G, Markowitz GS, Li L, D'Agati VD, Factor SM, Geng L, Tibara S, Tuchman J, Cai Y, Park JH, van Adelsberg J, Hou H, Jr., Kucherlapati R, Edelmann W, Somlo S. Cardiac defects and renal failure in mice with targeted mutations in pkd2. *Nature genetics*. 2000;24:75-78
3. Moyer JH, Lee-Tischler MJ, Kwon HY, Schrick JJ, Avner ED, Sweeney WE, Godfrey VL, Cacheiro NL, Wilkinson JE, Woychik RP. Candidate gene associated with a mutation causing recessive polycystic kidney disease in mice. *Science (New York, N.Y.* 1994;264:1329-1333
4. Okada H, Bakal C, Shahinian A, Elia A, Wakeham A, Suh WK, Duncan GS, Ciofani M, Rottapel R, Zuniga-Pflucker JC, Mak TW. Survivin loss in thymocytes triggers p53-mediated growth arrest and p53-independent cell death. *The Journal of experimental medicine*. 2004;199:399-410
5. Takakura A, Contrino L, Beck AW, Zhou J. Pkd1 inactivation induced in adulthood produces focal cystic disease. *J Am Soc Nephrol*. 2008;19:2351-2363
6. Claxton S, Kostourou V, Jadeja S, Chambon P, Hodivala-Dilke K, Fruttiger M. Efficient, inducible cre-recombinase activation in vascular endothelium. *Genesis*. 2008;46:74-80
7. Yang L, Besschetnova TY, Brooks CR, Shah JV, Bonventre JV. Epithelial cell cycle arrest in g2/m mediates kidney fibrosis after injury. *Nature medicine*. 2011;16:535-543, 531p following 143
8. Wang Y, Krishna S, Golledge J. The calcium chloride-induced rodent model of abdominal aortic aneurysm. *Atherosclerosis*. 2013;226:29-39
9. Patel V, Li L, Cobo-Stark P, Shao X, Somlo S, Lin F, Igarashi P. Acute kidney injury and aberrant planar cell polarity induce cyst formation in mice lacking renal cilia. *Human molecular genetics*. 2008;17:1578-1590
10. Lanoix J, D'Agati V, Szabolcs M, Trudel M. Dysregulation of cellular proliferation and apoptosis mediates human autosomal dominant polycystic kidney disease (adpkd). *Oncogene*. 1996;13:1153-1160
11. AbouAlaiwi WA, Ratnam S, Booth RL, Shah JV, Nauli SM. Endothelial cells from humans and mice with polycystic kidney disease are characterized by polyploidy and chromosome segregation defects through survivin down-regulation. *Human molecular genetics*. 2011;20:354-367
12. Nauli SM, Alenghat FJ, Luo Y, Williams E, Vassilev P, Li X, Elia AE, Lu W, Brown EM, Quinn SJ, Ingber DE, Zhou J. Polycystins 1 and 2 mediate mechanosensation in the primary cilium of kidney cells. *Nature genetics*. 2003;33:129-137
13. AbouAlaiwi WA, Takahashi M, Mell BR, Jones TJ, Ratnam S, Kolb RJ, Nauli SM. Ciliary polycystin-2 is a mechanosensitive calcium channel involved in nitric oxide signaling cascades. *Circulation research*. 2009;104:860-869
14. Nauli SM, Kawanabe Y, Kaminski JJ, Pearce WJ, Ingber DE, Zhou J. Endothelial cilia are fluid shear sensors that regulate calcium signaling and nitric oxide production through polycystin-1. *Circulation*. 2008;117:1161-1171

15. Abdul-Majeed S, Nauli SM. Dopamine receptor type 5 in the primary cilia has dual chemo- and mechano-sensory roles. *Hypertension*. 2011;58:325-331
16. Amores A, Postlethwait JH. Banded chromosomes and the zebrafish karyotype. *Methods in cell biology*. 1999;60:323-338
17. Rothschild SC, Francescatto L, Drummond IA, Tombes RM. Camk-ii is a pkd2 target that promotes pronephric kidney development and stabilizes cilia. *Development*. 2011;138:3387-3397
18. Obara T, Mangos S, Liu Y, Zhao J, Wiessner S, Kramer-Zucker AG, Olale F, Schier AF, Drummond IA. Polycystin-2 immunolocalization and function in zebrafish. *J Am Soc Nephrol*. 2006;17:2706-2718
19. Sun Z, Amsterdam A, Pazour GJ, Cole DG, Miller MS, Hopkins N. A genetic screen in zebrafish identifies cilia genes as a principal cause of cystic kidney. *Development*. 2004;131:4085-4093

SUPPLEMENTAL MOVIE LEGENDS

Movie S1. Normal cell division in renal epithelial cell.

The movie shows a cell undergoing a normal mitotic event. The movie was analyzed by superimposing DIC and Hoechst fluorescence images, which were taken every five minutes with 40X magnification.

Movie S2. Failure of cytokinesis induced polyploidy formation in survivin knockdown renal epithelial cell.

The movie shows that abnormal cytokinesis leads to polyploidy formation. The survivin knockdown cell is able to initiate cell division but is unable to execute cytokinesis properly. The cell then shows various membrane blebbing followed by the formation of a cytomegalic cell with multiple nuclei. Images were captured every two minutes with 40X magnification.

Movie S3. Normal cell division in vascular endothelial cell.

The movie shows a cell undergoing a normal mitotic event. The movie was analyzed by superimposing DIC and Hoechst fluorescence images, which were taken every two minutes with 40X magnification.

Movie S4. Failure of cytokinesis induced polyploidy formation in survivin knockdown vascular endothelial cell.

The movie shows that abnormal cytokinesis leads to polyploidy formation. The survivin knockdown cell is able to initiate cell division but is unable to execute cytokinesis properly. The cell then shows various membrane blebbing followed by the formation of a cytomegalic cell with

multiple nuclei. Of note is the presence of another multinucleated cell within the field of view. Images were captured every two minutes with 40X magnification.